A New Strategy for Multifunction Myoelectric Control using an Array of Surface Electrodes

by

Sentiono Leowinata
B.Sc., University of Prince Edward Island, 1995

A Thesis Submitted in Partial Fulfillment of
The Requirements for the Degree of

Master of Science in Engineering

in the Graduate Academic Unit of
Electrical and Computer Engineering

Supervisors: Bernard S. Hudgins, Ph. D., Biomedical Engineering
Philip A. Parker, Ph. D., Electrical Engineering

Examining Board: Rajamani Doraiswami, Ph. D., Electrical Engineering
Kevin B. Englehart, Ph. D., Electrical Engineering
Brandford, G. Nickerson, Ph. D., Computer Science

THE UNIVERSITY OF NEW BRUNSWICK

September 2000

Peace in the World

"You can if you think and you believe you can"

Abstract

One of the limitations of current multifunction myoelectric control systems is the amount of myoelectric signal data required to classify with a reasonable accuracy the signals to be used as a control input. The amount of data required introduces a time delay in the myoelectric control systems which hinders the development of a continuous type of control. A new strategy is proposed to handle this limitation by employing an array of surface electrodes and correlation feature vector. The aim is to develop a new strategy which can make a reasonably accurate decision faster than the mechanical response of the systems. An array of surface electrodes, placed around the targeted group of muscles, gives a broader and more complete characterization of the myoelectric signal for each type of contraction. The information captured by each channel is computed by correlation methods to form a correlation feature vector. The patterns exhibited by the correlation feature vector are used as an input to classifiers. A total of five basic classifiers were employed to test the strategy on simulated and real myoelectric signals data and results are presented. Using four myoelectric channels and a 10-feature vector, the strategy can provide input to the classifiers to reasonably classify six basic hand movements with as little as 50 ms of steady-state data. This shows that the update rate of the strategy is faster than the mechanical response of current prostheses limbs.

Acknowledgments

It is impossible to name every person that contributes to the writing of this thesis. However, I sincerely thank every one for realizing this thesis. The most deserving people are my two supervisors, Dr. Bernard S. Hudgins and Dr. Philip A. Parker. Thank you for your complete trust, endless patience and support, and invaluable advice and guidance throughout the course of the research program. I thank Dr. Hudgins and Dr. Parker for giving me the opportunity to study, work and research with you. I would like to express my sincere thanks to Dr. R. Doraiswami for his input and ideas throughout this research.

I would like to extend my gratitude to the staff and faculty of the Institute of Biomedical Engineering for their assistance and friendship. In particular, I would like to thank Mr. J. Hayden and Dr. D. Lovely for ther assistance in technical matters, Dr. B. Caldwell, Ms. D. Stocker, Mr. G. Bush, Mr. W. Young, Mr. P. Paasche, and Mr. M. Olive for their advice and input from a practical point of view, and Ms. K. Copp and Ms. A. Hamilton for their assistance on finding research materials. I would like to thank the students of the Institute for all discussions on all topics and warm relationships throughout my stay. In particular, I would like to thank Mr. John Landry for his editorial comments and friendship, Ms. D. MacIsaac for her friendship and input on many topics, and Mr. Gianluca deLuca and Mr. Jim Hunt for their advice on the topic. In would also like to thank the staff of Electrical and Computer Engineering, particularly Ms. D. Burke and Ms. S. Cormier for their assistance.

Last but not least, I want to thank my family and friends for their patience, love, encouragement, understanding, and total support, and for everything.

Table of Contents

List of Tables

List of Figures

LIST OF SYMBOLS AND ABBREVIATIONS

$\bar{Z}(m)$	correlation feature vector
$\bar{H}(m)$	cross-correlation element of the feature vector
$\bar{P}(m)$	autocorrelation element of the feature vector
$\Omega_m(i,j)$	cross-correlation coefficient of i and j channels with $i \neq j$ for the m^{th} class
$\omega_m(i)$	autocorrelation of the i^{th} channel for the m^{th} class
$R_{ij}^{m}(\tau)_{peak}$	peak value of cross-correlation between channel i and j for the m^{th} class
$R_{ii}^{m}(\tau)_{peak}$	peak value of autocorrelation of the i^{th} channel for the m^{th} class
μ_m	mean of the m^{th} class
Σ_m	covariance of the m^{th} class
AP	action potential
AR	autoregressive
CNS	central nervous system
ECG	electrocardiogram
EMG	electromyography or electromyogram
MAV	mean absolute value
MEC	myoelectric control
MES	myoelectric signal
MUAP	motor unit action potential
SNR	signal-to-noise ratio

Chapter 1

Introduction

1.1. Background

A muscle is made from fibers which change their state when they are excited by the nerves. When a muscle fiber is excited, it generates a signal known as the action potential (AP) [1], [2]. A signal generated as a result of the stimulation of a group of muscle fibers by a common nerve axon is a motor unit action potential (MUAP). The spatial and temporal summation of many MUAPs is a myoelectric signal (MES) [1]. The MES is typically measured with electrodes and the information gathered is known as an electromyogram (EMG). A more detailed discussion on the MES is provided in Chapter 2.

Myoelectric control (MEC) is a control strategy for powered artificial limbs that employs the MES as the control input. As in any control strategy, the reliability of the control system depends on the input. The reliability of the MEC depends on the success of decoding the MES into reliable and distinguishable patterns. Unfortunately, decoding MES into distinct patterns to be used as input is difficult due to the characteristics of the signal. The unique interaction between MEC and the MES is explored in Chapter 2.

The idea of employing MEC for powered prostheses had been suggested as early as late 19th century. However, lack of understanding and knowledge about the MES prevented practical implementation until Reiter demonstrated a working MEC system in

1948 [3]. The combination of Reiter's work and an increased demand for prostheses after World War II encouraged many researchers to investigate MEC further.

Coupled with the improved knowledge in human physiology which provides a deeper understanding of the MES, many countries, including England, Germany and Russia, competed to build better MEC systems [4]. In 1960, Kobrinsky expanded Reiter's work by showing that the method can be utilized to control prosthetic devices [5]. Kobrinsky's work was further enhanced by Dorcas and Scott from the University of New Brunswick (UNB) who developed a three-state MEC system which is now known as the UNB system [6].

In recent years, the advancements in computer technology have allowed further development of MEC. In 1991, Hudgins proposed a new multifunction MEC system using an artificial neural network to extract information patterns from the MES. This system provided proportional five-state control [7]. Today, there are two principal approaches to MEC: state (level coded) based and pattern (feature coded) based. Current MEC systems are addressed in Chapter 2.

1.2. Problem Definition

Although both state-based and pattern-based approaches have offered improved functionality and reliability since the inception of MEC, there is a common limitation. Both strategies require a large amount of MES data (> 200 ms) to achieve a reasonable classification accuracy.

The amount of data required by existing systems introduces a time delay in the

selection of a prosthesis function. This time delay hinders the development of a continuous type of control where the input to the control system is required to be faster than or at least equal to the response of the system. Therefore, it is required to find a way to make the update rate faster than or equal to the mechanical response of MEC systems to achieve a continuous type of control.

1.3. Objectives

The general objective of the research is to develop a strategy to solve the above common limitation of multifunction MEC. The specific objective of the research is to reduce the time required for the selection of a function with a reasonable classification accuracy. To ensure that the strategy is adhered to, the following criteria have been devised:

- The classification performance of the new strategy must be as good as or better than the current systems when using the same amount of MES data.
- The MES data required for the system to select a function must allow an update rate equal to or faster than mechanical response of MEC systems.
- The control strategy must be based on voluntary and natural contractions.
- The system must adapt to user's needs and require minimum training.

It is crucial that the classification performance of the proposed strategy be as good as or better than the current system with equivalent data, and exceed those performance levels with less data. It is expected that the method offered in this research will meet these criteria and provide a starting point for continuous control.

1.4. Thesis Outline

Chapter 1 gave a brief background on MES and its relation to MEC. This chapter also showed an evolution of MEC, discussed the common problem that exists in current systems, and stated the objectives of the research.

Chapter 2 explains the generation of MES and its characteristics. It also provides a review of the relevant literature on MEC.

Chapter 3 presents the details of the proposed MEC strategy, followed by verification using simulated data. Also, classification results from four different classifiers are presented.

Chapter 4 demonstrates the performance of the method on real MES data. Various tests and approaches to validate the technique are also demonstrated.

Chapter 5 provides a summary of the results and discussion. As in any research, opening a new horizon will produce more questions than answers. This chapter also includes suggestions for future work.

Chapter 2

Background and Literature Review

2.1. Myoelectric Signal

A muscle is made from many muscle fibers which change their state when excited by the nerves [1]. The change generates electrical activity because of electrochemical processes in the fiber which cause the fiber to depolarize along the axis of the muscle. This resulting signal can be recorded by surface electrodes. Details on the depolarization of muscle fibers caused by nerve excitation can be found in any human physiology textbook or in [1], [2], [8] and [9].

The signal generated as a result of fiber depolarization is known as the action potential (AP). When a single nerve innervates a common group of muscle fibers known as a motor unit, the resulting signal generated by this group is called the motor unit action potential (MUAP). The spatial and temporal superposition of many MUAPs is a myoelectric signal (MES) [1]. An example of this superposition is shown in Figure 2.1.

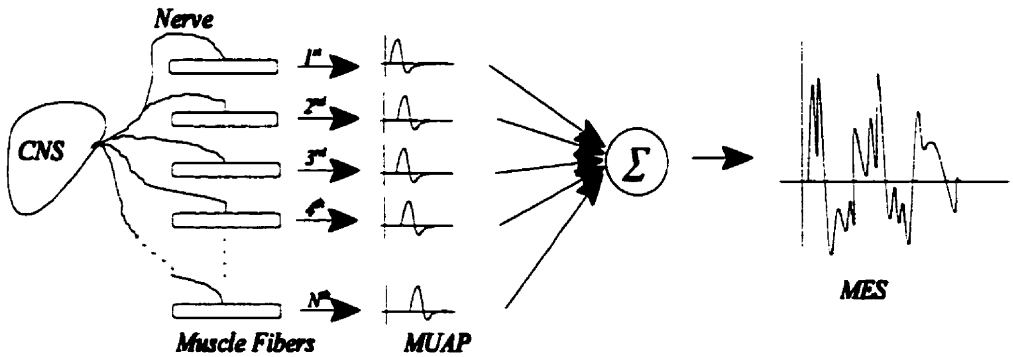

Figure 2.1. - Generation of Myoelectric Signal (MES)

Since the MES is a summation of many asynchronous firings, the MES has been modeled as a stochastic process [1], [9]-[12]. This random nature is more apparent when the MES is recorded by surface electrodes due to the pooled activity of the motor units within the pickup regions [7]. The recorded MES is also affected by tissue layers that exist between the muscle and the skin where the recording surface electrodes are placed. These tissue layers attenuate and exert a low pass filtering effect on the MES [13]. The random nature of the MES and the tissue filtering effect on the MES make the analysis of the MES difficult [7], [9], [14], [15].

2.2. Myoelectric Control

Hammond once said:

> "Designers of artificial limbs cannot hope to replace all the channels carrying information between muscles and the central nervous system lost through amputation. However, the application of control theory and modern electronics is helping to produce reliable artificial limbs which can even adapt slightly to their environment" [16].

There are two methods of acquiring control information of electrophysiological origin for artificial limbs. The first one is from the neural input [17] and the second one is from myoelectric signals [18]. Although measuring the neural input is possible [17], this technique is experimental and not clinically acceptable at present. The MES is an accepted way of acquiring control information for artificial limbs. Thus, only control strategies using MES as input, known as MEC, will be considered.

There are two ways to obtain MES: using surface electrodes and using intramuscular electrodes. Intramuscular electrodes have been used in the study of MES but are impractical for clinical applications. Surface electrodes have also been used in

clinics and laboratory experiments because they are non-invasive and the subjects experience less discomfort. Therefore, only MES obtained from surface electrodes is discussed. Unfortunately, the advantages of MES acquired by surface electrodes do not come without penalty. As identified in Section 2.1, the MES obtained using this method has a random nature and is affected by tissue filtering. In addition, the recording electrodes contribute noise to the signal [19], [20]. The combination of the random nature, the tissue filter, and noise makes the MES a complex signal and difficult to classify. Therefore, strategies to extract the patterns borne in the MES and classify them reliably are crucial before the signal can be used as input for the control systems. As a result, the reliability of MEC depends on the strategy used to classify patterns in the MES.

In general, there are two principal approaches in MEC systems: state (level coded) based and pattern (feature coded) based. Early MEC systems relied on the estimation of the amplitude [6] or the rate of amplitude change of the MES [21] to select a state or a function of the device. Once the state of the system is selected, the speed of the device can be proportionally controlled [18]. These systems are sufficient for controlling devices with one function (i.e. hand open) or at most two functions (i.e. hand open - hand close) but insufficient to control multifunction devices [7], [22], [23].

To provide multifunction control, more inputs from MES to the electromechanical system are needed. One method is to develop a strategy to extract patterns contained in the MES [23]-[25]. Many classification strategies have been proposed to provide more inputs to be used by MEC. Saridis and Gootee demonstrated that parameters in the MES such as signal zero crossing, signal variance and higher moments of the signal can be

used to control the prosthetic arm [23]. They used statistical analysis to classify combinations of six primitive functions (humeral rotation in, humeral rotation out, elbow flexion, elbow extension, wrist pronation, and wrist supination) and the linear discriminant was chosen as a classifier to test their strategy. Saridis and Gootee found that information provided by signal zero crossing and signal variance gave the best result for simple motions. Unfortunately, the strategy achieved only 65% classification rate when 170 ms of MES data sampled at 3 KHz was used. However, their work showed that there are indeed classifiable patterns in the MES.

In another approach, Scott showed that MES spectra contain useful control information [26]. Extending Scott's work, Graupe proposed a time-series model. An autoregressive (AR) model was developed [27] and was able to classify the MES into four to six different basic limb functions with 99% success rate after the subjects were trained for 12 hours to produce the parameters required [28]. This work was very promising but no reported work was able to reproduce the results. Moreover, with computing power available at that era, the time required to process the MES data (2.5 s) was impractical. Furthermore, the burden imposed on the subjects is not acceptable.

There was a pause in the development of MEC until 1991 when Hudgins proposed a new strategy for multifunction myoelectric control using an artificial neural network [7]. He used the MES mean absolute value (MAV), mean absolute value slope, zero crossings, slope changes, and waveform lengths as the features to determine the limb functions. Four different limb functions (elbow flexion, elbow extension, medial rotation of the humerus, and lateral rotation of the humerus) were used to test the strategy. The

average classification rate achieved was approximately 91% for normally-limbed subjects and approximately 86% for amputee subjects with 200 ms of MES data. These findings sparked a new interest in MES classification for MEC.

Extending Hudgins' work, Englehart used time-frequency features to classify myoelectric signals [22], [29]. Similar to Hudgins work, four limb functions (flexion and extension of the elbow, and pronation and supination of the forearm) determined from MES of the biceps and triceps were used to test the strategy. The average classification rate was 93.75% for normally-limbed subjects with 256 ms of MES data.

All the work mentioned above use either one or two MES channels to obtain control information. Work on multi-channel (array based) systems is discussed in the next section.

2.3. Array Based Myoelectric Signal and Myoelectric Control

Linear arrays of surface electrodes placed along the direction of the muscle fibers have been used for many years to measure conduction velocity and to localize motor units [30]-[35]. Hogan and Mann placed four pairs of differential electrodes over the belly of the biceps to estimate the MES amplitude [36], [37]. The electrodes were stainless steel disks, 12.7 mm in diameter, spaced longitudinally at 35 mm centers and laterally at 14 mm centers. They showed that more than 90% improvement in signal-to-noise ratio (SNR), where the $SNR = \left[\frac{E\{F\}^2}{E\{(\hat{F} - F)^2\}} \right]^{\frac{1}{2}}$, can be achieved when this array configuration was employed. Their results are corroborated by Clancy and Hogan who used eight electrodes placed side by side latitudinally across the biceps brachii and triceps

muscles to record the MES. Clancy and Hogan showed that multiple sites in this configuration improve the SNR for MES amplitude estimation up to 180% [38]. Their results encouraged researchers to implement arrays for other applications.

It was suggested that multiple electrodes would provide a broader and more complete MES characterization than a single channel since more information could be captured by the array. Doerschuk *et al.* used an array of four electrodes to extend the work of Graupe and Cline to find patterns in MES [39]. These patterns were discriminated by analyzing the time history of all limb-function probabilities. By viewing the discrimination problem as a statistical decision problem, a linear and time invariant AR model was proposed as

$$y(k) = \sum_{j=1}^{p} A_{m,j} y(k-j) + e_m(k); \quad m = 1,...,M$$

where $y(k)$ is the observed $L \times 1$ vector of the MES, p is the order of the model (p = 4), $\{A_{m,1}, ..., A_{m,p}\}$ are $L \times L$ coefficient matrices, $e_m(k)$ is the one-step-ahead prediction error vector, subscript m is the limb-function being modeled, M is the number of limb functions, and L is the number of electrodes. All information borne in the MES, including the crosstalk, was used to discriminate the signals. Six different limb functions (wrist flexion, wrist extension, wrist abduction, wrist adduction, forearm supination, and forearm pronation) each divided into four different phases (rest, initiation of function, hold, and return to rest by reversing the movement) for each function were used to test the AR model. Although the proposed model classified the six functions reasonably well, no

classification rate was given and no further research to extend this novel work can be found.

2.4. A New Strategy

All the control strategies described above require approximately 200 ms of MES data to extract the patterns from the signal. This amount of time is considered as the minimum time necessary to get a reliable estimate of the characteristics of the MES. The condition is true especially when the strategy employed (i.e. AR parameters) is very sensitive to disturbances [7], [23], [25].

With motivation (1) to investigate further the approach by Doerschuk *et al.*, (2) to reduce the time needed for pattern classification, and (3) to develop a continuous type of control for a prosthesis, a new strategy is proposed. The strategy will try to distinguish patterns in the MES by analyzing all of the information captured by the array including the crosstalk since it had been shown that the crosstalk contains useful information to discriminate functions [26], [27], [39]. Further discussion of the proposed new strategy is found in Chapter 3.

Chapter 3

A New Strategy

3.1. Methodology

The myoelectric control strategy outlined in this chapter is entirely new and consists of two parts. Firstly, a modified linear array of surface electrodes is used to obtain data. Instead of being placed along the muscle fiber, the array is placed around the arm of a subject. Secondly, the myoelectric signal obtained by the array is processed to form a correlation feature vector. The patterns exhibited by the vector identify the user's intent and are used as the control input for the prosthesis.

This technique was tested both on a set of simulated MES data and real MES data obtained from volunteer subjects. Analysis of the data and the results are performed both quantitatively and qualitatively. Performances of the method on a set of simulated data are presented in Sections 3.2 and 3.3, while results of the strategy on real MES data are discussed in Chapter 4.

3.1.1. Array of Surface Electrodes

A linear array of surface electrodes has been used and is accepted as one of the standards for measuring the conduction velocity of a muscle. The array is normally placed along the direction of muscle fiber as shown in Figure 3.1.

The new strategy modifies the placement of the electrodes by positioning the array

around the targeted group of muscles as shown in Figure 3.2. This configuration allows greater signal capture as the muscles contract to perform various movements.

Figure 3.1. Array along the Muscle Fiber
(adopted and modified with permission, Gray, p. 370 [40])

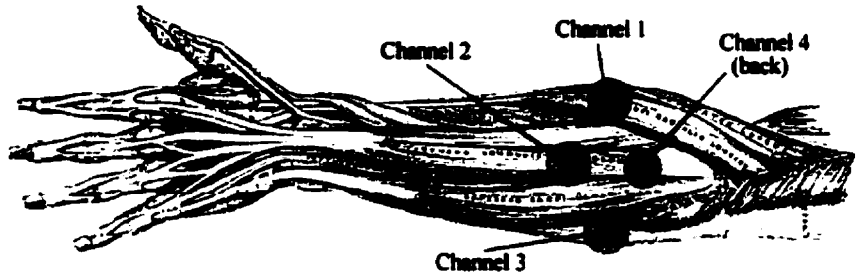

Figure 3.2. Modified Array Configuration
(adopted and modified with permission, Gray, p. 370 [40])

As mentioned in Section 2.1, the MES obtained by surface electrodes is affected by tissue filtering and often interfered with by other signals such as electrocardiogram (ECG), motion artifact, interference from the power source (60 Hz or 50 Hz), skin stretch potentials, cable and electrode capacitive effects. The situation is worsened when the electrodes are used in an array configuration. The array configuration captures not only signals from different channels simultaneously but also records crosstalk among channels [10], [12], [14], [27], [38], [39].

Many researchers view crosstalk as another form of noise which does not contain useful information. However, a few researchers have demonstrated that crosstalk can

improve the performance when it is properly used [38], [39]. The author believes that crosstalk can be exploited to enhance pattern discrimination since it carries useful information such as the relative activity of the muscles performing certain movements. The array of surface electrodes as shown in Figure 3.2 is a plausible choice as it increases the amount of signal information including the crosstalk without sacrificing either time needed to capture the information or patient comfort.

3.1.2. Correlation Feature Vector

Cross-correlation and autocorrelation functions can provide spectral information and 2nd order moments of signals [41], [42]. The correlation method is used extensively in biological signal processing for the measurement of the conduction velocity of a muscle. A typical approach is to compute the cross-correlation of the channels of the array. The time delays exhibited by the computation show the propagation velocity of the signal as it travels along the fibers of the muscle being monitored [35].

A signal classification problem typically looks for certain characteristics in a given set of signals to segregate the signals into a number of classes. The correlation method can also be used to discriminate signals since it also provides useful information. Doerschuk *et al.* demonstrated that autocorrelation and cross-correlation features can be exploited to discriminate patterns in the MES [39]. The author believes that information captured by correlations of the MES has unique features which can be put to use as a basis for pattern classification. If these unique features are captured and used to create patterns for each functional movement, it is possible to use the correlations for pattern

classification and as the input for the myoelectric control system.

As stated in the objective, the strategy must be able to make a reasonably accurate decision that is faster than the current MEC systems. To do that, the amount of MES data must be obtained in less than 200 ms without sacrificing the information content. Rich information exhibited by correlation methods may be able to capture such information with short data records. Autocorrelation of each channel gives a measure of relative activity which has been used to develop a simple three-degree-of-freedom control [43]. However, this measure has insufficient information for more complex systems where several functions are to be controlled. Cross-correlations among channels in the array, on the other hand, may exhibit some consistent patterns for particular activities. A method is therefore required to capture these patterns by using characteristics such as the power in each channel, and the cross-powers, to enable decision making in a shorter time than the current MEC systems.

Introducing a new feature vector, called $\bar{Z}(m)$ *or* $Z(m)$, which is defined as follows

$$\bar{Z}(m) = \begin{bmatrix} \bar{H}(m) \\ \bar{P}(m) \end{bmatrix} \qquad (1)$$

where the $\bar{H}(m)$ and $\bar{P}(m)$ are defined as

$$\bar{H}(m) = \frac{1}{\max(\Omega_m(i,j))} \left[\Omega_m(i,j) \right] \qquad (2a)$$

$$\bar{P}(m) = \frac{1}{\max(\omega_m(i))} \left[\omega_m(i) \right] \qquad (2b)$$

where $\Omega_m(i,j)$ is the cross-correlation coefficient of i and j channels with $i \neq j$, $\omega_m(i)$ is the autocorrelation of i^{th} channel of the array, and m is the class. The $\bar{H}(m)$ and $\bar{P}(m)$ correlation vectors can be updated continuously to give a measure of change in the activity. The correlation feature vector $\bar{Z}(m)$ maps a path in the feature space which should be related to the continuous intent of the user. The correlation coefficients expressed above are computed from

$$\Omega_m(i,j) = \frac{R_{ij}^m(\tau)_{peak}}{\sqrt{R_{ii}^m(\tau)_{peak}} * \sqrt{R_{jj}^m(\tau)_{peak}}} \quad where \ i \neq j; \qquad (3a)$$

and

$$\omega_m(i) = R_{ii}^m(\tau)_{peak} = R_{ii}^m(0) \qquad (3b)$$

where $R_{ij}^m(\tau)_{peak}$ is the peak value of the cross-correlation between channel i and channel j, and $R_{ii}^m(\tau)_{peak}$ is the peak value of the autocorrelation of the i^{th} channel (the energy of the i^{th} channel). The $R_{ij}^m(\tau)_{peak}$, $R_{ii}^m(\tau)_{peak}$, and $R_{jj}^m(\tau)_{peak}$ are computed using Fast Fourier Transform method and the duration of the time record used are the data record length.

The classification problem is reduced to recognizing patterns in the lower dimension $\bar{Z}(m)$ vector rather than in the higher dimension myoelectric signals. The features exhibited in the vector represent user intent and, assuming that different feature vectors exist for different intent, this information can be used as the function selection of the control system. A system diagram that describes this relationship is shown in Figure 3.3. The results given in Chapter 4 demonstrate that such patterns exist for real MES.

The next sections describe the results for simulated MES data.

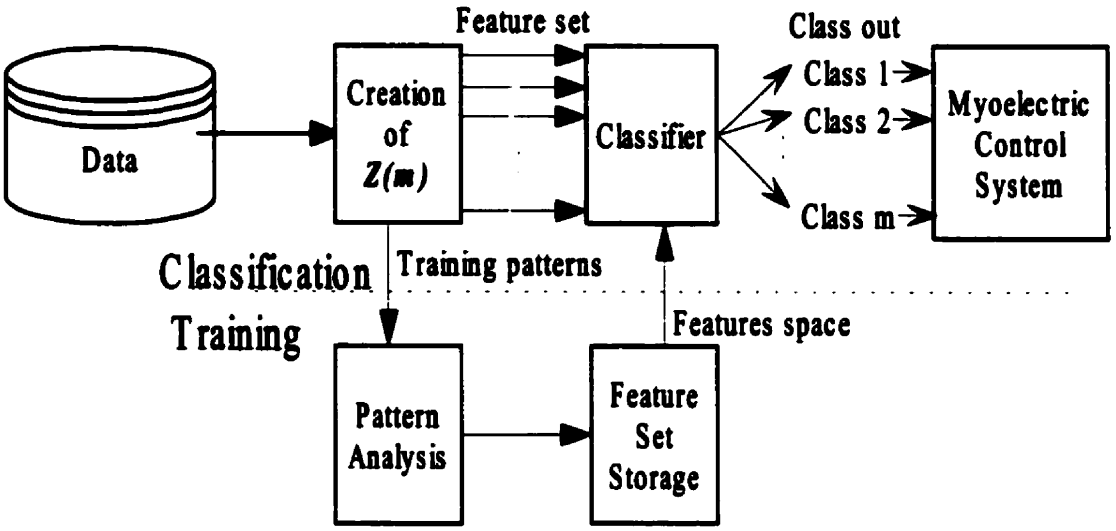

Figure 3.3. - Relationship between User Intent and Myoelectric Control System (adopted and modified with permission, Hudgins [7])

3.2. Verification of the Strategy on a Set of Simulated MES Data

The strategy's ability to correctly identify signals with short MES data records was tested using simulated data. A model was developed to simulate the acquisition of Gaussian distributed MES from an array of four surface electrodes. A Gaussian distribution was chosen since the MES obtained from surface electrodes are Gaussian distributed [9]. The objective was to classify the simulated MES into three distinct patterns. Modeling of the MES in this manner is done only to test the concept. It is by no means assumed or implied that this simulated data accurately models real MES data. It is used for test purposes only since accurately modeling surface MES from a number of active muscles has been shown to be a difficult task.

3.2.1. Generation of Simulated MES Data

Two sets of Gaussian random signals with zero mean and unity variance were generated using Matlab 4.2c. These random signals were band-limited to dc-1000 Hz and were considered to be the simulated MES of two identical active muscles as recorded at the muscle surface. The third signal was generated from a weighted combination of those two signals. Each signal was generated one-thousand times to make one-thousand realizations. An example of a signal, generated using this simulation method, is shown in Figure 3.4.

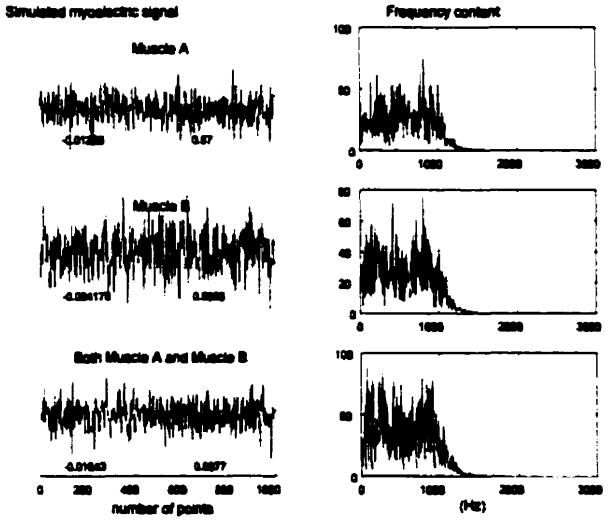

Figure 3.4. - A Sample of Simulated MES Data

The generated MES was filtered and scaled before being used to test the strategy. Figure 3.5 illustrates the position of the electrodes and the effect of the tissue filters on the simulated MES data. Four 4th-order Butterworth band-pass filters with different bandwidths were produced using Matlab 4.2c to simulate the aspect of tissue filtering that

exists between each muscle and each recording electrode site. The four filters had 3 dB bandwidths of 20-180 Hz, 20-110 Hz, 20-140 Hz, and 20-200 Hz respectively. After filtering, the signals were also scaled accordingly to reflect signal attenuation due to the distance from the source to each of the electrodes. Attenuation factors A-H range from 1 when the muscle source is considered active to 0.1 when it is not active. These values were obtained through experimental measurements from one normally-limbed subject with electrodes configuration as in Figure 3.5 placed on biceps and triceps. Table 3.1 tabulates the combinations of the filters and the weighting factors that were used to model the signal recorded at each electrode for the three possible muscle activity patterns.

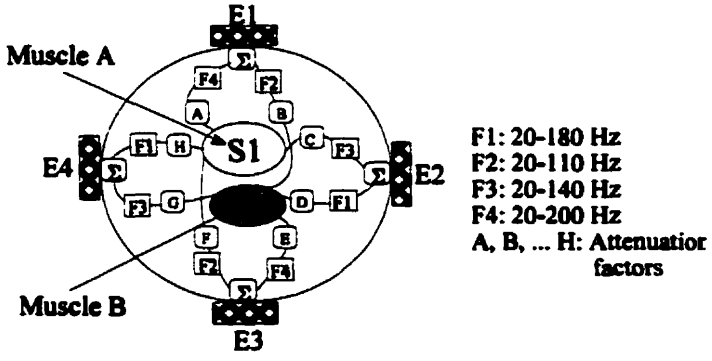

Figure 3.5. - Illustration of Electrode Array and Tissue Filter Effect for Simulated MES Data

Muscle Activity Pattern	Signals Recorded at Electrode Location			
	E1	E2	E3	E4
Muscle A	(F4*S1) + (F2*0.1*S2)	(0.955*F3*S1) + (F1*0.1*S2)	(0.338*F2*S1) + (F4*0.1*S2)	(0.332*F1*S1) + (F3*0.1*S2)
Muscle B	(F4*0.1*S1) + (0.470*F2*S2)	(F3*0.1*S1) + (0.670*F1*S2)	(F2*0.1*S1) + (F4*S2)	(F1*0.1*S1) + (0.802*F3*S2)
Muscle A + B	(F4*S1) + (0.470*F2*S2)	(0.955*F3*S1) + (0.670*F1*S2)	(0.338*F2*S1) + (F4*S2)	(0.332*F1*S1) + (0.802*F3*S2)

Table 3.1. - Combination of Weighting Factors and Bandpass Filters to Simulate Three Distinct Patterns from Two Sources

3.2.2. Classifiers Employed

Since there were three different signals to be classified and the array consisted of four surface electrodes, the m^{th} contraction type vector is

$$\bar{z}(m) = [\Omega_m(1,2)\ \Omega_m(1,3)\ \Omega_m(1,4)\ \Omega_m(2,3)\ \Omega_m(2,4)\ \Omega_m(3,4)\ \omega_m(1)\ \omega_m(2)\ \omega_m(3)\ \omega_m(4)] \quad m = 1,2,3$$

where the correlation coefficients were computed using Equations 3a and 3b for i and j = 1,...,4.

Once the parameters of the correlation feature vector were established, techniques to classify the signals were required. Four classifiers were employed to classify these three signals. These classifiers were the rank order, the minimum distance (Euclidean distance measure), the Bayes quadratic discriminant, and the fuzzy c-means.

3.2.2.1. The Rank Order Classifier

The method used for the rank order classifier is very simple. It classifies the signals based on the pattern shown by the index of the feature vector after they have been sorted in ascending order of amplitude. The values in the feature vector for each of the one thousand realizations are computed and ranked in ascending order. After ranking, only the order is relevant since the amplitude information is lost. The index of the structure forms a unique pattern where the signals are clustered into different classes. At this point, the last five coefficients of the ordered vector were taken as the class specific pattern. A vector of more than five coefficients did not improve the classification and indeed the added noise in the vector often caused poor classification results. Similarly, if

fewer coefficients were taken, insufficient information was available to classify the signals. A sample Matlab 4.2c program is included in Appendix C (CD-ROM).

3.2.2.2. The Minimum Distance (Euclidean) Classifier

The minimum distance classifier discriminates the signals based on Euclidean distance. The distance of a given vector is computed without any weight factors against the center (mean) of established classes.

$$\min_{m} \left\{ (\bar{Z}-\mu_m)^T (\bar{Z}-\mu_m) \right\}, \qquad m = 1,2,3$$

where $\mu_m = E[\overline{Z}_1(m)]$ is the mean-value of each class obtained from a training set. The decision that a vector belongs to a particular class is determined by the smallest distance.

It is necessary to determine a training set and a test set for each of the classes, since a mean value for each class must be established. The first five-hundred realizations were used as the training set and the next five-hundred realizations as the test set. Sample of Matlab 4.2c code to perform these calculations is included in Appendix C (CD-ROM).

3.2.2.3. The Bayes Quadratic Discriminant Classifier

Since the simulated MES data has a Gaussian distribution, the decision rule of the Bayes quadratic discriminant can be expressed by

$$\max_{m} \left\{ \frac{1}{(2\pi)^{\frac{N}{2}} |\Sigma_m|} \exp^{\left[-\frac{1}{2}(\bar{Z}-\mu_m)^T \Sigma_m^{-1} (\bar{Z}-\mu_m)\right]} \right\} \qquad m = 1,2,3$$

where N is the dimension of the correlation feature vector $\bar{Z}(m)$ (i.e. 10 or 16 for 4 MES channels), $\Sigma_m = E[(\bar{Z}_i(m)-\mu_i)^T(\bar{Z}_j(m)-\mu_j)]$ is the covariance matrix, $|\Sigma_m|$ is the determinant, and $\mu_m = E[\bar{Z}_1(m)]$ is the mean-value of each class obtained from a training set, $\bar{Z}_1(m)$.

The training data used the first five-hundred realizations to determine the covariance and the mean for each class. The next five-hundred realizations were used as the test data. A sample Matlab 4.2c program to perform these calculations is included in Appendix C (CD-ROM).

3.2.2.4. The Fuzzy c-Means Classifier

The fourth classifier was the fuzzy c-means classifier. Fuzzy c-means can tolerate contradictions that often exist due to the random nature of the MES. The ability to handle contradictions is an advantage over the previous three classifiers and one of the reasons this classifier was selected. The decision criteria is to minimize the sum-of-squared errors function [44]

$$J_m(U,\underline{v}_i) = \sum_{k=1}^{n} \sum_{i=1}^{c} (U_{ik})^m (d_{ik})^2$$

where

$$\underline{v}_i = \frac{\sum_{k=1}^{n} (U_{ik})^m \underline{x}_k}{\sum_{k=1}^{n} (U_{ik})^m}, \quad i = 1,\ldots,c$$

$$u_{ik} = \frac{1}{\sum_{j=1}^{c} \left(\frac{d_{ik}}{d_{jk}}\right)^{\frac{2}{m-1}}}, \quad I_k = \varnothing = \textit{nullset}$$

$$u_{ik} = 0 \quad I_k \neq \varnothing \ \textit{and} \sum_{i \in I_k} u_{ik} = 1$$

$$I_k = \{i \mid 1 \leq i \leq c;\ d_{ik} = \|\underline{x}_k - \underline{v}_i\| = 0\}$$

where $\underline{x}_k$ is the input vector, U_{ik} is the fuzzy membership, and d_{ik} is the Euclidean norm between $\underline{v}_i$ and $\underline{x}_k$. More detailed explanation of the equations can be found in [44] and [45].

The value of c (partition index) was chosen to be three since three signals were to be classified. The fuzziness (degree of uncertainty/confusion) of the classifier is controlled by the value of m (fuzziness index). Although the fuzziness index can take any value between $1 \leq m < \infty$, the index was chosen to be 2. This value is the recommended value in literature when a fuzzy classifier is compared to non-fuzzy classifiers such as the three previous classifiers [44], [45]. The initial membership function $U^{(0)}$ ($U^{(0)} \in M_{fc}$), where M_{fc} stands for the membership of fuzzy classifier, for each class is determined from the apriori knowledge of the MES pattern which was obtained from the rank order technique. An arbitrary weight (certainty value) is assigned to each feature element to make the complete membership function. The values of the weights are critical. If the

initial membership function is assigned randomly, it will result in a poor classification accuracy. The value of $U^{(o)}$ was chosen as follows

$$U^{(0)} = \begin{bmatrix} 0.70 & 0.50 & 0.85 & 0.07 & 0.45 & 0.06 & 0.95 & 0.02 & 0.00 & 0.32 \\ 0.15 & 0.40 & 0.10 & 0.86 & 0.45 & 0.09 & 0.00 & 0.02 & 0.96 & 0.36 \\ 0.15 & 0.10 & 0.05 & 0.07 & 0.10 & 0.85 & 0.05 & 0.96 & 0.04 & 0.32 \end{bmatrix}$$

where the first two rows are the initial weighting factor for muscle A and muscle B, and the last row is the initial weighting factor when both muscle A and muscle B are active (co-contraction).

The first five-hundred realizations were taken as a training set where the data was used to compute the c-fuzzy clusters $\{\underline{v}_i^{(l)}\}$ and the subsequent membership function $U^{(l)}$. As the computation progressed in the loop, the values of $U^{(l)}$ and $\{\underline{v}_i^{(l)}\}$ were updated.

Once the membership function and c-fuzzy clusters had been updated by the training set, the fuzzy c-means classified the next five-hundred realizations. The implementation of this classifier followed Bezdek's algorithm [44]. A sample program in Matlab 4.2c code is included in Appendix C (CD-ROM).

3.3. Performance of the Strategy on Simulated MES Data

The classification rates (in percent) of the four different classifiers for different data record sizes are summarized in Figure 3.6 and tabulated in Table 3.2. All classifiers classified the simulated signals into three different classes with >90% accuracy if the sampled data was sufficiently long (i.e. $n > 200$). The rank order classifier gives the poorest results for reasonable data records (i.e. $n < 200$). The Bayes quadratic

discriminant, the minimum distance, and the fuzzy c-means all yielded 100% accuracy using 200 points of simulated MES data and give reasonable classification rates with as little as 30 points of simulated MES data.

# of sample points	5	10	20	30	40	50	100	200	500	1000
Rank Order	32.8	39.0	50.4	55.9	60.0	60.6	75.7	90.4	99.5	100
Min. Distance	77.0	80.1	88.9	93.4	95.7	97.3	99.7	100	100	100
Quad. Discriminant	79.3	83.1	90.1	96.3	99.3	99.7	100	100	100	100
Fuzzy c-Means	78.7	85.1	93.7	97.1	98.4	99.1	99.6	100	100	100

Table 3.2. - Classification Rate (in percent) of Different Strategies for Different Data Record Length on Simulated MES Data

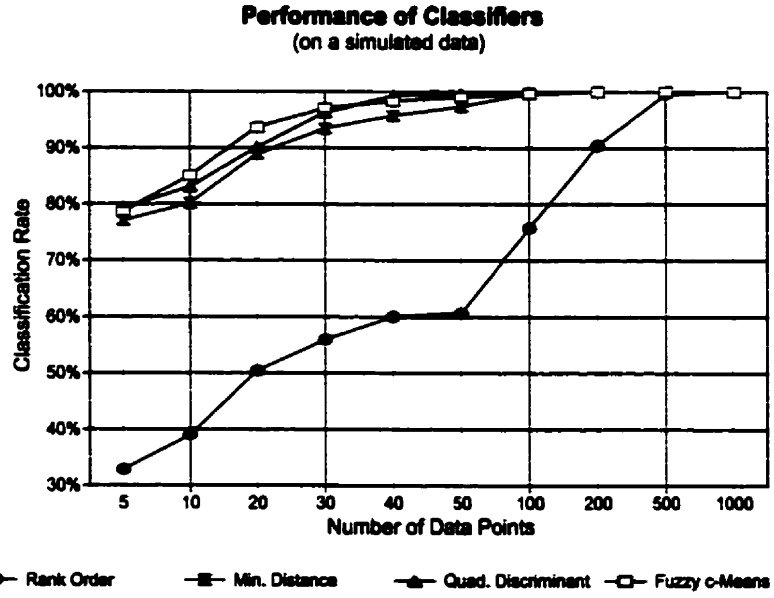

Figure 3.6. - Performance of Different Classifiers for Different Data Record Length

Since the sampling rate used was 1000 Hz (1 point = 1 ms), the results of this simulation show that only a short data record (i.e. 30 ms) is needed to estimate the control

input reasonably. If similar results can be obtained from real MES data, the strategy can be used in continuous myoelectric control. Thus, further investigation was undertaken to test the technique on real MES data. This is presented in the next chapter.

The rank order and the fuzzy c-means classifiers were omitted in the analysis of the real MES data. The rank order classifier was dropped due to its poor performance on the simulated data. The rank order could classify the signals with >90% accuracy only when the input data was 200 ms or more. The fuzzy c-means classifier gave the best performance giving 93% classification accuracy with as little as 20 ms of simulated MES data. However, the minimum distance and the Bayes quadratic discriminant performed nearly as well (90%) with 20 ms of simulated MES data. In addition, the fuzzy c-means classifier depends on the assigned values in the initial membership function. Assigning the values for the initial membership function would be very difficult and time consuming as it is subject dependent. Furthermore, choosing random values for the initial membership function in the Bezdek's fuzzy c-means will yield poor performance. Therefore, there appears to be little advantage to using a more complex classifier such as fuzzy c-means over the Bayes quadratic discriminant and the minimum distance classifiers. Thus, the fuzzy c-means classifier was left for future work.

Chapter 4

Performance of The Strategy with Real Myoelectric Signals

4.1. Data Acquisition

Chapter 3 showed that the new strategy which uses an electrode array and a correlation feature vector was able to identify the simulated signals with high classification accuracy with as little as 30 ms of simulated MES data. To confirm that the method can be used in myoelectric control, it must be tested on real MES data.

Twelve volunteer subjects, eleven normally-limbed and one with a congenital limb deficiency, were recruited. Each subject read and signed an informed consent form (a sample of the consent form is included in Appendix B) before the experiment began. The subjects were reminded during the experiment that they were free to withdraw at anytime without any obligations. The subjects were asked to perform six basic upper-limb (hand) movements as illustrated in Figure 4.1: finger flexion, finger extension, wrist flexion, wrist extension, ulnar deviation and radial deviation. The amputee subject was asked to visualize the same hand movements and perform them to the best of the subject's ability.

Figure 4.1. - Illustration of Six Different Movements

The complexity of the correlation feature vector $\bar{Z}(m)$ depends on the number of MES channels in the array. It was hoped that four myoelectric channels would be sufficient to classify six basic hand movements while keeping the feature vector simple and not computationally intensive. Therefore, an array that consisted of four myoelectric channels was used to acquire the MES data. However, it does not mean that the feature vector $\bar{Z}(m)$ is limited to four channels. When more complex movements are going to be investigated, the features in the $\bar{Z}(m)$ vector may be increased by having more channels in the array. The optimum number of channels in the array given a set of contractions is left for future work.

An array of four surface electrodes was positioned around the arm of the subjects (see Figure 3.2 for illustration). The array was placed in such a way that each channel monitored either different active regions of the muscles (normally-limbed subjects) or so that they were well separated with equal spacing between the electrodes (limb deficient subject). No attempt was made to optimize the position of the array. The optimum placement of the array is left for future work.

The data from each channel was amplified by a standard opto-isolated amplifier with a common mode rejection ratio greater than 100 dB. The amplified signals were simultaneously recorded at 1000 points per second (1 point = 1 ms) by a DAS 16/330 A/D board that was attached to an IBM PC 486. In-house software, written in C and LabView, was used for data acquisition. A block diagram of the data acquisition process is shown in Figure 4.2.

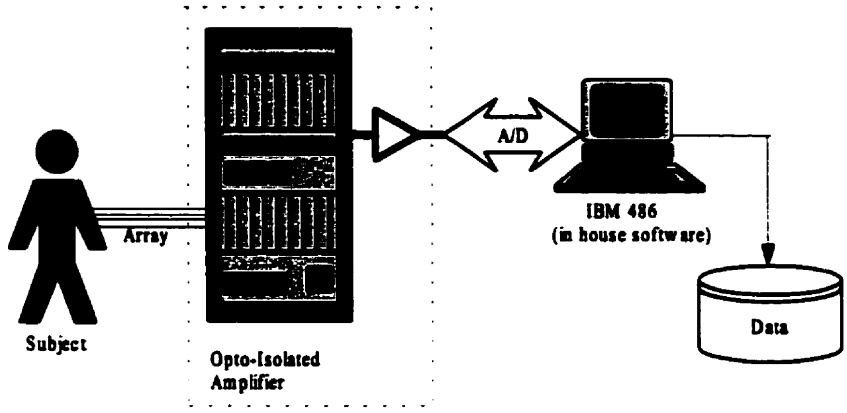

Figure 4.2. - Block Diagram of the Data Acquisition

4.2. Myoelectric Signal Data

Two types of MES data were investigated in order to determine the performance of the strategy. The first data type was transient signals obtained from muscles that were recruited from a relaxed state to an excited state. Hudgins, in his Ph.D. thesis, successfully demonstrated that the first 256 ms of MES data contained specific (deterministic) patterns for different types of contractions [7]. This was corroborated by the recent finding of Englehart who extended the analysis of the transient MES into the time-frequency domain [22]. Based on the findings of Hudgins and Englehart, the proposed strategy was tested on the transient signals to evaluate its performance. Figure 4.3(a) shows an example of the transient signals measured in each of the four MES channels as the muscles go from a relaxed to an active state and back to a relaxed state.

The second data type was from steady-state signals. Steady-state data were obtained during a relatively isometric/isotonic contraction as shown in Figure 4.3b.

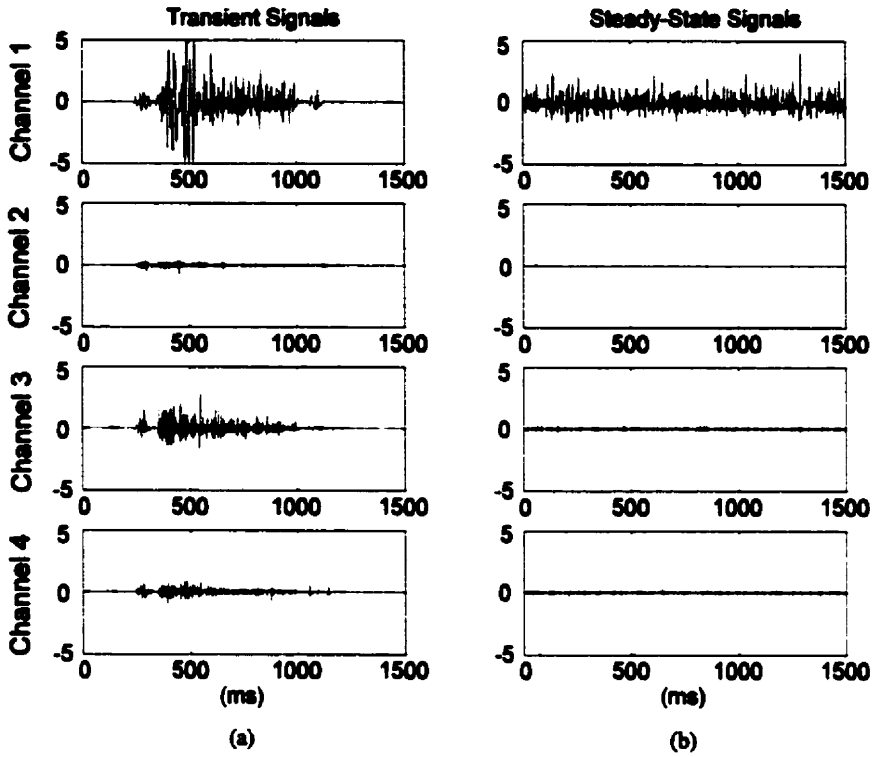

Figure 4.3. An Example of (a) Transient Signals, (b) Steady-State Signals from Each of the Four Channels.

Initially, the transient data was obtained using a monopolar configuration. The placement of the array in a monopolar configuration is shown in Figure 4.4. It was postulated that this arrangement would give an accurate measure of the activity from each electrode site. However, it was difficult to find a common reference site for the monopolar configuration. There is a possibility that the common mode signals could mask signals from the recording channels if the reference site is placed on active muscles. The problem was confirmed when the data collected from one subject showed that a large common mode component was measured by each channel. Therefore, this configuration was abandoned and replaced by a bipolar configuration. The bipolar configuration shown

in Figure 4.5 was used to collect all other MES data.

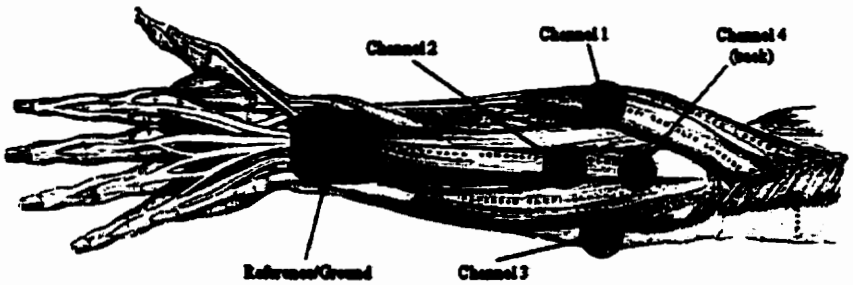

Figure 4.4. Array with Monopolar Configuration
(adopted and modified with permission, Gray, p. 370 [40])

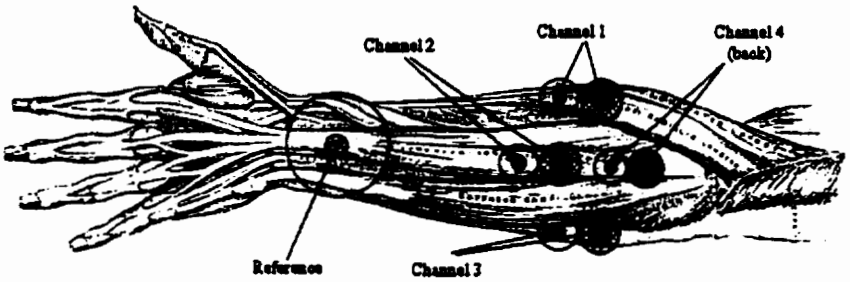

Figure 4.5. Array with Bipolar Configuration
(adopted and modified with permission, Gray, p. 370 [40])

In obtaining the steady-state data, subjects were asked to hold one of the six hand movements for approximately sixty seconds while the data was recorded from the four channel array. Qualitative analysis was performed to ensure that the captured information contained none of the initial transient signals.

Since one of the research's objectives is to develop a strategy that requires a shorter time to make a control decisions in a more continuous manner, analyzing steady-state data is more crucial than investigating the transient data. Testing the strategy with steady-state data can confirm if the method is usable as a starting point for the development of a continuous MEC system.

4.3. Data Analysis

Three classifiers were used in the analysis of the real MES data. Two classifiers, the Bayes quadratic discriminant and the minimum distance, which were used to test the simulated data, were used again in the analysis of the real data. The real MES data was considered to have a Gaussian distribution so that the Bayes quadratic discriminant could be used as a classifier [9]. The third classifier, the linear discriminant, was added as a bridge between the Bayes quadratic discriminant and the minimum distance classifier. The Bayes quadratic discriminant classifier includes the covariances of each class. Although these separate considerations might bring more accurate representation of the characteristics of each class, the strict conditions imposed by the Bayes quadratic discriminant might yield singularities on certain classes during training. On the other hand, the minimum distance classifier does not consider the covariance from each class in its classification membership function. The linear discriminant maintains the information by averaging the covariance from all classes. This reduces the computational complexity. Therefore, the linear discriminant was chosen as the third classifier.

In the following sections, the analysis of the data is discussed and is broken into two main parts. First, the performance of the strategy on the transient data is discussed. Different settings and combinations of strategy parameters (i.e. threshold window size in which the number of data points used in threshold calculation, data record length, and features of the correlation vector) were tested with the three different classifiers, are explored and discussed. Second, the performance of the strategy on the steady-state data is presented. Similar to the first part, various tests with different settings on the steady-

state data were performed and the results are discussed. For both types of data, the first fifty percent was used as the training set while the last fifty percent was used as the test set.

4.3.1. Analysis with the Transient Data

It is important to note that the initiation of the signals must be captured in order to classify the transient signals correctly [7]. If the starting point is captured too early, the signal contains noise with no MES information. If the beginning of the signals is not obtained, then the deterministic patterns in the transient signals are not captured. A qualitative analysis coupled with a simple algorithm was used to determine the starting point of the transient signals. The algorithm used the mean absolute value (MAV) of the noise level of each channel. A value of three times the MAV of the noise level was used as the threshold. When the MAV of the signals from any of the four channels exceeded the threshold, the contraction was assumed to start. In addition, a qualitative analysis was performed on every signal and was used as a guide when the simple threshold algorithm failed to detect the initiation point which could happen for a very low level contraction.

For every transient data record from every subject, the record length (amount of data or time duration), the threshold window size, and the features of the $\bar{Z}(m)$ vector were varied with each classifier. The record length was varied from 1024 to 10 ms. The threshold window size used six different settings which are 50, 25, 20, 15, 10, and 5 ms. The $\bar{Z}(m)$ vectors were either normalized in which the $\bar{H}(m)$ and the $\bar{P}(m)$ were calculated as

$$\bar{H}(m) = \frac{1}{\max(\Omega_m(i,j))}\left[\Omega_m(i,j)\right] \quad or \quad \bar{H}(m) = \frac{1}{\max|\Omega_m(i,j)|}\left[\Omega_m(i,j)\right]$$
$$\bar{P}(m) = \frac{1}{\max(\omega_m(i))}\left[\omega_m(i)\right] \quad or \quad \bar{P}(m) = \frac{1}{\max|\omega_m(i)|}\left[\omega_m(i)\right]$$

or not normalized in which case the $\bar{H}(m)$ and the $\bar{P}(m)$ were computed as

$$\bar{H}(m) = \left[\Omega_m(i,j)\right] \quad or \quad \bar{H}(m) = \left|\left[\Omega_m(i,j)\right]\right|$$
$$\bar{P}(m) = \left[\omega_m(i)\right] \quad or \quad \bar{P}(m) = \left|\left[\omega_m(i)\right]\right|$$

Since the data was obtained from four electrodes, the $\bar{Z}(m)$ vector can have either 10 features or 16 features. A vector of ten features was created from the combination of the six cross-correlation features of the $\bar{H}(m)$ and the four autocorrelation features of the $\bar{P}(m)$. A vector of sixteen features was made from these 10 features plus the delays associated with the cross-correlation between each channel. The combination of the features of the $\bar{Z}(m)$ (10 or 16 features), the threshold window size (50, 25, 20, 15, 10, 5 ms) and the record length (1024, 512, 256, 200, 100, 50, 40, 30, 20, 10 ms) was tested on the Bayes quadratic discriminant, the linear discriminant, and the minimum distance classifiers resulting in a total of 1920 tests. Only results from the normalized feature vector are presented and discussed. Results from the non-normalized feature vector can be found in Appendix C (CD-ROM). The programs and the results from all subjects for all combinations performed are included in Appendix C (CD-ROM).

Figures 4.6, 4.7, and 4.8 show the classification rate of the Bayes quadratic

discriminant[1], the linear discriminant, and the minimum distance classifiers for six classes (hand movements) as the record length was varied with a threshold window size of 25, and the $\bar{Z}(m)$ vector had 10 features normalized to the maximum value only. Figure 4.9 compares the average performance of each classifiers employed over all subjects for six classes.

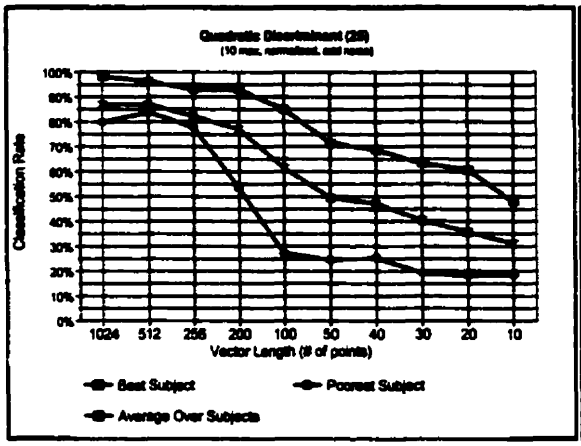

Figure 4.6. - Classification Rate of the Quadratic Discriminant for Six Classes

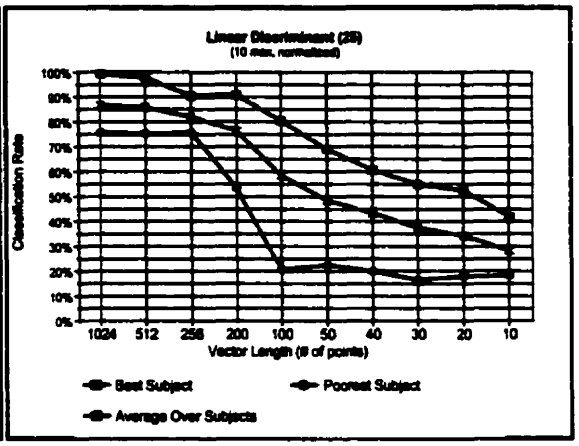

Figure 4.7. - Classification Rate of the Linear Discriminant for Six Classes

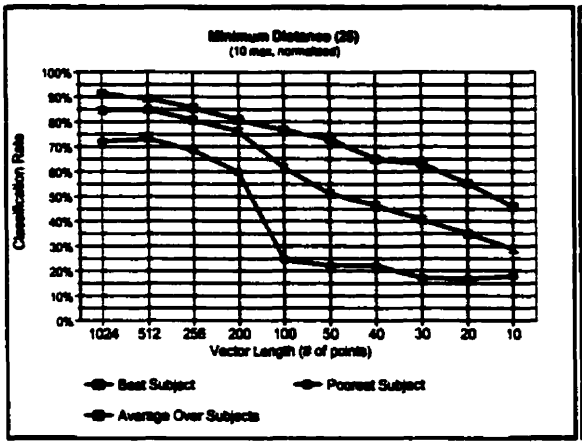

Figure 4.8. - Classification Rate of the Minimum Distance for Six Classes

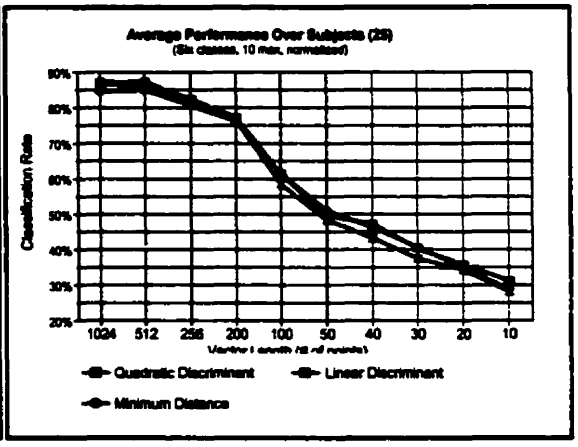

Figure 4.9. - Average Classification of Each Classifier over All Subjects for Six Classes

[1]A small noise was added to prevent singularity for the Bayes quadratic discriminant

The results from the best subject, the average over subjects, and the worst subject from nine normally-limbed subjects are shown in Figures 4.6, 4.7, 4.8 and 4.9.

As shown by the graphs, the performance of the strategy in classifying the MES data is respectable. Furthermore, with 200 ms of MES data the performance of the best subject when six classes with ten-feature vector (93.4%) was tested by the quadratic discriminant is comparable to the performance of the best subject on Hudgins' work which classified fewer classes (four limb functions) with 30 features (98%) [7]. However, the strategy showed a significant performance degradation when it tried to classify the transient signal with less than 200 ms of MES data. The significant decline in the classification performance when the input data is less than 200 ms is also shown by Hudgins and Englehart when they tried to classify four classes [7], [22]. Furthermore, there is little difference in performance for the different classifiers. This suggests that 200 ms is the minimum amount of MES data required to classify the transient signals with a reasonable accuracy.

Results from 16-feature vector (available in Appendix C on CD-ROM) also showed that the performance degraded significantly when the data record length used was less than 200 ms. These results also show that the higher dimension (16-feature) vector did not improve the classification performance over the 10-feature vector. This means that including the time delay terms in the feature vector did not add any new information. Therefore, the 16-feature vector was no longer used.

Figures 4.10, 4.11, and 4.12 demonstrate the effect of the threshold window size on the average performances of the Bayes quadratic discriminant, the linear discriminant

and the minimum distance classifiers when the $\bar{Z}(m)$ vector used 10 features normalized to the maximum value only.

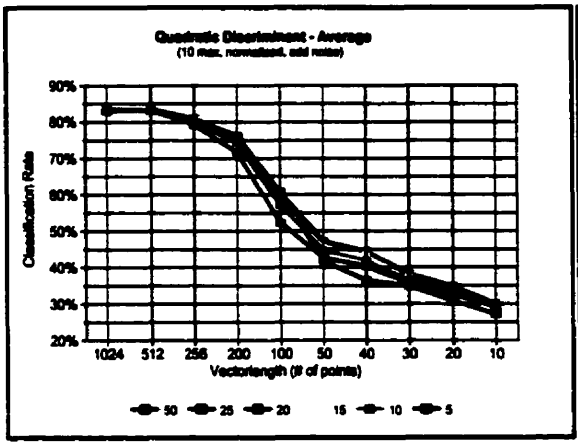

Figure 4.10. - Effect of the Threshold Window Size on the Average Performance of the Quadratic Discriminant for Six Classes

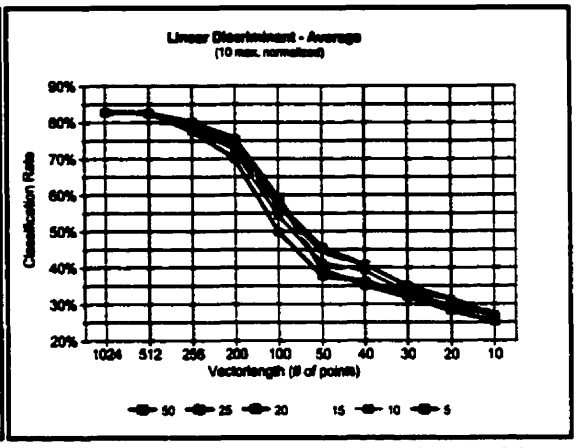

Figure 4.11. - Effect of the Threshold Window Size on the Average Performance of the Linear Discriminant for Six Classes

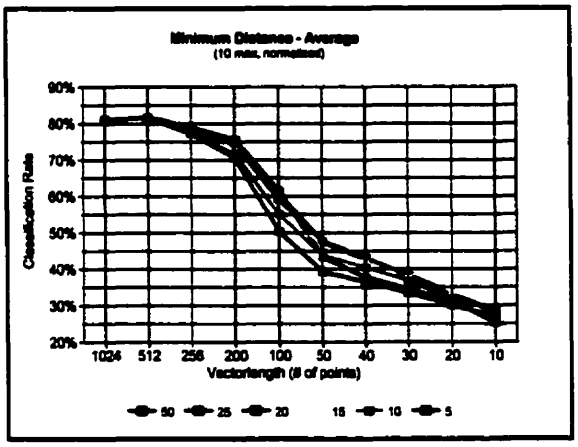

Figure 4.12. - Effect of the Threshold Window Size on the Average Performance of the Minimum Distance Discriminant for Six Classes

Although the window size of 25 shows the best classification rate overall, it is clear from the graphs that the window size has little effect on the performance of the strategy from

the graphs. The performance degradation is also evident from the Figures 4.10, 4.11 and 4.12 when the strategy tried to classify the transient signal with less than 200 ms of MES data. All other results on the effect of the threshold window size of different combinations are included in Appendix C (CD-ROM).

4.3.2. Analysis with the Steady-State Data

The steady-state data was analyzed differently from the transient data. The threshold window size was dropped since no starting point needed to be found. The $\overline{Z}(m)$ vector used 10 features where the $\overline{H}(m)$ and the $\overline{P}(m)$ were either normalized in which case they were calculated as

$$\overline{H}(m) = \frac{1}{\max(\Omega_m(i,j))}\left[\Omega_m(i,j)\right] \quad with \quad \overline{P}(m) = \frac{1}{\max(\omega_m(i))}\left[\omega_m(i)\right]$$

or not normalized in which case the $\overline{H}(m)$ and the $\overline{P}(m)$ were calculated as

$$\overline{H}(m) = \left[\Omega_m(i,j)\right] \quad with \quad \overline{P}(m) = \left[\omega_m(i)\right]$$

Again, the same three classifiers were used to test the performance of the strategy on the steady-state data.

4.3.2.1. Performance of the Steady-State Data

Six different tests were performed to analyze the steady-state data from nine

normal-limbed subjects. Results from the Bayes quadratic discriminant[2] (Q. D.) are shown in Figures 4.13 and 4.14. Results from the linear discriminant (L. D.) are shown in Figures 4.15 and 4.16, while results from the minimum distance (M. D.) are given in Figures 4.17 and 4.18. Again, only results from the best subject, the average over all subjects and the poorest subject are shown in the graphs for clarity. All other results can be found in Appendix C (CD-ROM).

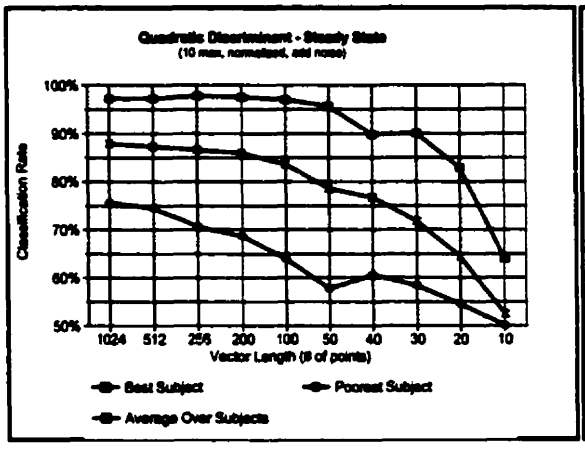

Figure 4.13. - Classification Rate of the Normalized Q. D. for Six Classes

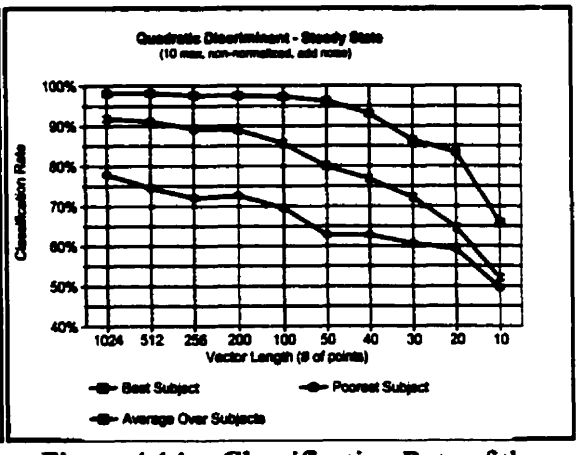

Figure 4.14. - Classification Rate of the Non-Normalized Q. D. for Six Classes

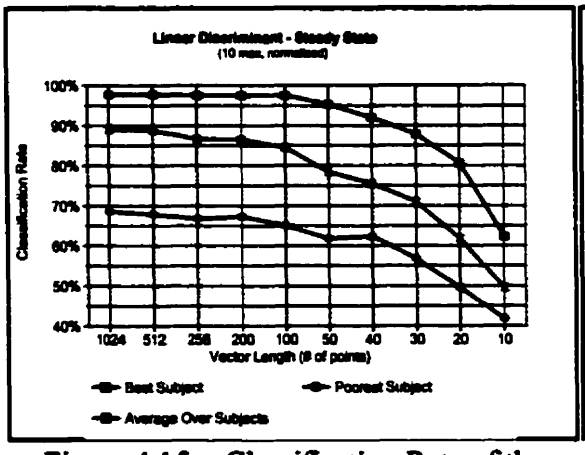

Figure 4.15. - Classification Rate of the Normalized L. D. for Six Classes

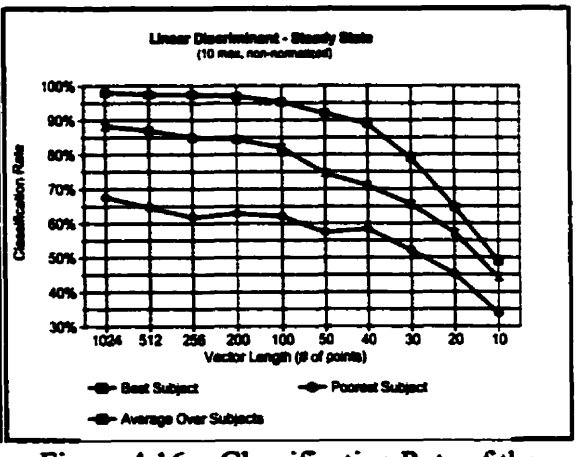

Figure 4.16. - Classification Rate of the Non-Normalized L. D. for Six Classes

[2]A small noise was added to prevent singularity for the Bayes quadratic discriminant

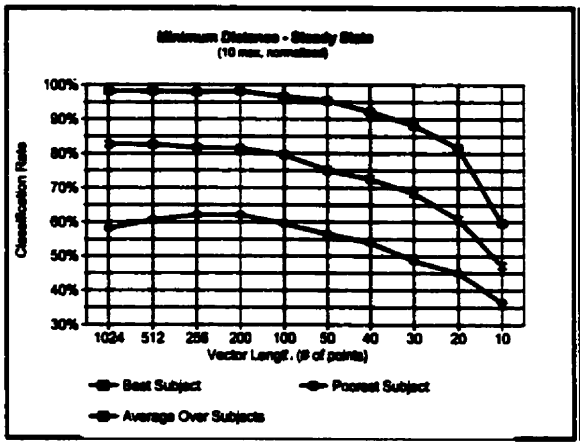

Figure 4.17. - Classification Rate of the Normalized M. D. for Six Classes

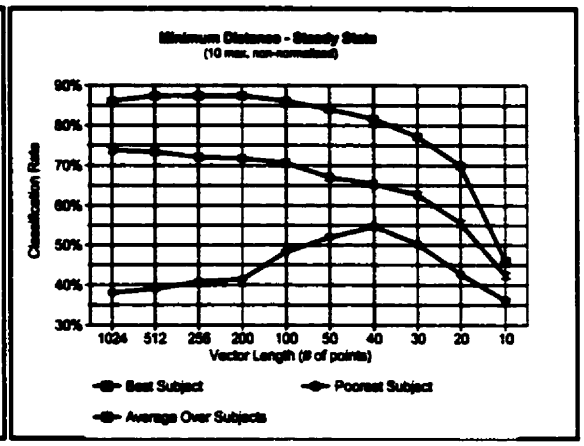

Figure 4.18. - Classification Rate of the Non-Normalized M. D. for Six Classes

As shown by the graphs, the strategy can classify six classes (hand movements) with a high degree of classification accuracy up to 200 ms of MES data. Furthermore, the technique can classify six classes with as little as 50 ms of MES data with less than a 10% drop in the performance. This finding is significant considering all the data was obtained from untrained subjects. In addition, the performance of the normalized feature vector (Figures 4.13, 4.15, and 4.17) are more consistent than the non-normalized feature vector (Figures 4.14, 4.16, and 4.18). This means that the patterns exhibited by the normalized feature vector are more stable than the non-normalized vector since the ratio are kept approximately the same. However, the non-normalized vector also has some advantage in that the relative strength (force) information is retained. This information is very useful if a proportional control is desired (although a simple MAV measure can be used as well). The normalized and the non-normalized feature vector can be coupled to produce one system. The normalized feature vector can be used to classify the signals by maintaining the consistency while the non-normalized feature vector can be used to control the speed.

This investigation and other possible use of the non-normalized feature vector are left for future work.

On the other hand, although the Bayes quadratic discriminant gave a better performance when the feature vector was not normalized (Figure 4.14) and the performances of the linear discriminant classifier for the normalized (Figure 4.15) and the non-normalized (Figure 4.16) cases are almost identical, there are negative effects of this non-normalized feature vector. A detrimental effect of this non-normalized feature vector on the classification performance is shown by Figure 4.18 where the minimum distance classifier was used. The performance of the minimum distance classifier drops more than 10% for the same amount of data when the feature vector is not normalized. Therefore, a non-normalized feature vector is not used for further analysis.

4.3.2.2. Performance of a Fixed Length Training Set

It was postulated that the larger the data record used for training, the higher the test set classification performance. Thus, a trial where the data record length of the training set was fixed at 1024 ms while the data record length test set was varied from 1024 to 10 ms was carried out. The experiment was run only on the normalized 10-feature $\bar{Z}(m)$ vector. Figure 4.19 shows the output of the Bayes quadratic discriminant, Figure 4.20 displays the result of the linear discriminant, and Figure 4.21 exhibits the outcome of the minimum distance. Figure 4.22 compares the performance of each classifier over all subjects when classifying six classes (hand movements) for fixed and variable training set data record length.

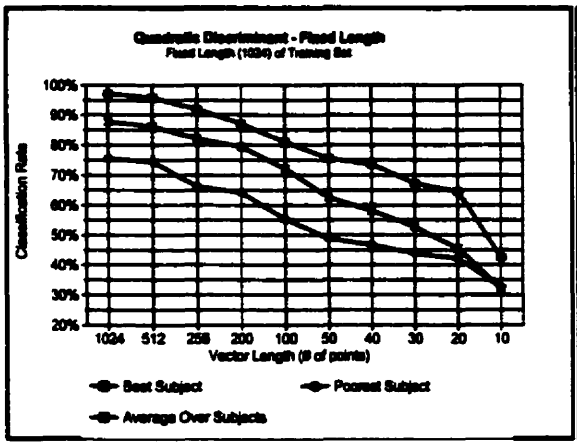

Figure 4.19. - Classification Rate of the Q.D. with a Fixed Length Training Set (1024) for Six Classes

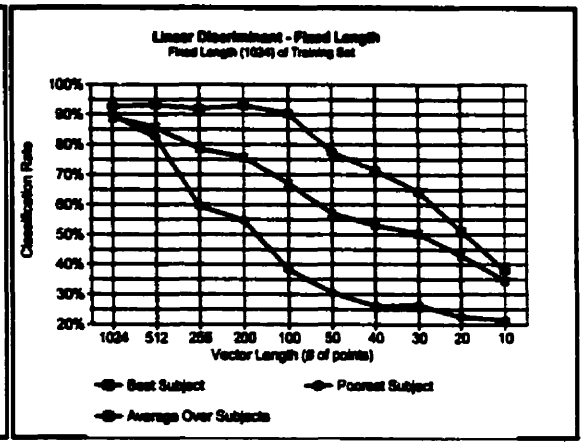

Figure 4.20. - Classification Rate of the L.D. with a Fixed Length Training Set (1024) for Six Classes

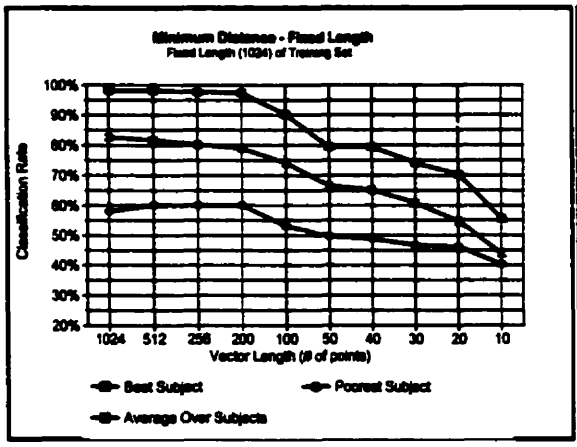

Figure 4.21. - Classification Rate of the M.D. with a Fixed Length Training Set (1024) for Six Classes

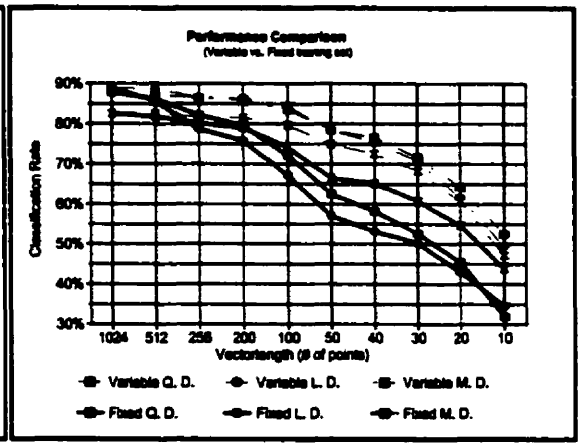

Figure 4.22. - Performance Comparison between Fixed Length Training Set and Variable Length Training Set

It is evident from Figure 4.22 that the fixed length training set approach constantly performs more poorly than the variable training data record length (results of fixed length training set are shown using the solid lines while the dashed-line represented results of variable length training set). This phenomena can be explained. The fixed length strategy used 1024 ms to train the classifier resulting in tightly bound classes with small variances. When test data with large variance was classified, the spread confused the classifier. The

classifier could not determine to which class the data belonged, since it was not trained to handle data with large variances. As a result, only the dominant classes could be classified correctly while the other classes were misclassified as one of the dominant class. Confusion matrices, showing how the other classes are misclassified and other results of the test, are included in Appendix C (CD-ROM).

4.4. Four Class Problem

The results previously shown were for the six class (six distinct hand movements) problem. If the confusion matrices are examined, it is clear that there are major and minor classes. These minor classes lowered the performance of the strategy. Examples of the confusion matrices from the Bayes quadratic discriminant with a variable length training set using the steady-state data are shown in Table 4.1a, 4.1b, 4.1c, 4.1d, 4.1e, and 4.1f. The rows give the record length of the input data while the columns are the classification accuracy and the classification error. The correct classification of Table 4.1a is finger flexion (F. F.) and the classification error column are the other five classes (hand movements). Table 4.1b, 4.1c, 4.1d, 4.1e, and 4.1f show the correct classification of the finger extension (F. E.), the wrist flexion (W. F.), the wrist extension (W. E.), the ulnar deviation (U. D.), and the radial deviation (R. D.) respectively.

Input Data (ms)	Finger Flexion	Error				
		W. F.	F. E.	R. D.	U. D.	W. E.
1024	100.0%	0.0%	0.0%	0.0%	0.0%	0.0%
512	100.0%	0.0%	0.0%	0.0%	0.0%	0.0%
256	100.0%	0.0%	0.0%	0.0%	0.0%	0.0%
200	100.0%	0.0%	0.0%	0.0%	0.0%	0.0%
100	100.0%	0.0%	0.0%	0.0%	0.0%	0.0%
50	100.0%	0.0%	0.0%	0.0%	0.0%	0.0%
40	98.3%	0.0%	0.0%	1.7%	0.0%	0.0%
30	93.3%	0.0%	0.0%	6.7%	0.0%	0.0%
20	83.3%	0.0%	3.3%	13.3%	0.0%	0.0%
10	76.7%	0.0%	13.3%	8.3%	0.0%	1.7%

Table 4.1a. - Classification Rate of Finger Flexion versus Data Record Sizes with Error Rate of Other Five Classes

Input Data (ms)	Finger Extension	Error				
		F. F.	W. F.	R. D.	U. D.	W. E.
1024	66.7%	0.0%	0.0%	33.3%	0.0%	0.0%
512	68.3%	0.0%	0.0%	31.7%	0.0%	0.0%
256	58.3%	0.0%	0.0%	41.7%	0.0%	0.0%
200	45.0%	0.0%	0.0%	53.3%	0.0%	1.7%
100	40.0%	0.0%	0.0%	60.0%	0.0%	0.0%
50	45.0%	1.7%	0.0%	48.3%	3.3%	1.7%
40	40.0%	5.0%	0.0%	41.7%	6.7%	6.7%
30	36.7%	8.3%	0.0%	41.7%	8.3%	5.0%
20	35.0%	3.3%	0.0%	43.3%	10.0%	8.3%
10	36.7%	11.7%	0.0%	20.0%	15.0%	16.7%

Table 4.1b. - Classification Rate of Finger Extension versus Data Record Sizes with Error Rate of Other Five Classes

Input Data (ms)	Wrist Flexion	Error				
		F. F.	F. E.	R. D.	U. D.	W. E.
1024	100.0%	0.0%	0.0%	0.0%	0.0%	0.0%
512	100.0%	0.0%	0.0%	0.0%	0.0%	0.0%
256	100.0%	0.0%	0.0%	0.0%	0.0%	0.0%
200	100.0%	0.0%	0.0%	0.0%	0.0%	0.0%
100	100.0%	0.0%	0.0%	0.0%	0.0%	0.0%
50	96.7%	3.3%	0.0%	0.0%	0.0%	0.0%
40	100.0%	0.0%	0.0%	0.0%	0.0%	0.0%
30	100.0%	0.0%	0.0%	0.0%	0.0%	0.0%
20	100.0%	0.0%	0.0%	0.0%	0.0%	0.0%
10	98.3%	0.0%	0.0%	0.0%	1.7%	0.0%

Table 4.1c. - Classification Rate of Wrist Flexion versus Data Record Sizes with Error Rate of Other Five Classes

Input Data (ms)	Wrist Extension	Error				
		F. F.	W. F.	F. E.	R. D.	U. D.
1024	13.3%	0.0%	0.0%	51.7%	35.0%	0.0%
512	6.7%	0.0%	0.0%	60.0%	33.3%	0.0%
256	8.3%	0.0%	0.0%	60.0%	31.7%	0.0%
200	16.7%	0.0%	0.0%	41.7%	41.7%	0.0%
100	21.7%	0.0%	0.0%	58.3%	20.0%	0.0%
50	15.0%	0.0%	0.0%	50.0%	33.3%	1.7%
40	23.3%	0.0%	0.0%	45.0%	30.0%	1.7%
30	36.7%	1.7%	0.0%	23.3%	33.3%	5.0%
20	28.3%	3.3%	0.0%	26.7%	35.0%	6.7%
10	26.7%	3.3%	0.0%	26.7%	25.0%	18.3%

Table 4.1d. - Classification Rate of Wrist Extension versus Data Record Sizes with Error Rate of Other Five Classes

Input Data (ms)	Ulnar Deviation	Error				
		F. F.	W. F.	F. E.	R. D.	W. E.
1024	76.7%	0.0%	0.0%	23.3%	0.0%	0.0%
512	86.7%	0.0%	0.0%	13.3%	0.0%	0.0%
256	81.7%	0.0%	0.0%	16.7%	0.0%	1.7%
200	75.0%	0.0%	0.0%	20.0%	1.7%	3.3%
100	65.0%	0.0%	0.0%	25.0%	5.0%	5.0%
50	38.3%	0.0%	0.0%	31.7%	18.3%	11.7%
40	43.3%	0.0%	0.0%	26.7%	15.0%	15.0%
30	28.3%	0.0%	0.0%	33.3%	20.0%	18.3%
20	31.7%	0.0%	0.0%	25.0%	25.0%	18.3%
10	25.0%	3.3%	0.0%	21.7%	16.7%	33.3%

Table 4.1e. - Classification Rate of Ulnar Deviation versus Data Record Sizes with Error Rate of Other Five Classes

Input Data (ms)	Radial Deviation	Error				
		F. F.	W. F.	F. E.	U. D.	W. E.
1024	96.7%	0.0%	0.0%	3.3%	0.0%	0.0%
512	85.0%	0.0%	0.0%	13.3%	0.0%	1.7%
256	75.0%	0.0%	0.0%	21.7%	0.0%	3.3%
200	75.0%	0.0%	0.0%	21.7%	0.0%	3.3%
100	56.7%	0.0%	0.0%	33.3%	0.0%	10.0%
50	51.7%	1.7%	0.0%	38.3%	1.7%	6.7%
40	58.3%	1.7%	0.0%	31.7%	3.3%	5.0%
30	55.0%	3.3%	0.0%	31.7%	1.7%	8.3%
20	48.3%	8.3%	0.0%	25.0%	5.0%	13.3%
10	36.7%	8.3%	0.0%	26.7%	15.0%	13.3%

Table 4.1f. - Classification Rate of Radial Deviation versus Data Record Sizes with Error Rate of Other Five Classes

From the tables, there are unclassifiable data sets even with 1024 ms of MES data. The dominant classes such as finger flexion and wrist flexion are classifiable with 100% accuracy when the input data is sufficient but suffer from misclassification as the data is shortened (shown by Table 4.1a and 4.1c). Tables 4.1b, 4.1d, 4.1e, and 4.1f show that certain contractions are confused with other classes even when the data is sufficient. The classification accuracy drops as the data is shortened.

The purpose of the test is to determine if the classification accuracy is improved by reducing the problem to four classes. Only steady-state data from three subjects was tested. To reduce the time and the analysis, the Bayes quadratic discriminant, the linear discriminant and the minimum distance classifiers with a variable length training set were used. The four major classes and the two minor classes were determined from the performance of the steady-state data. The minor classes were ignored and assumed to be one of the major classes. The choice of lumping a minor class with a major class was decided qualitatively.

The results of the Bayes quadratic discriminant, the linear discriminant and the minimum distance for four classes are exhibited in Table 4.2, Table 4.3, and Table 4.4. The six class performance is also shown for comparison.

Input Data Record Length (ms)	Subject #1		Subject #2		Subject #3	
	Average 6 classes	Average 4 classes	Average 6 class	Average 4 class	Average 6 classes	Average 4 classes
1024	86.4%	100.0%	80.28%	98.75%	90.56%	99.58%
512	85.8%	100.0%	77.50%	95.42%	91.11%	100.00%
256	86.7%	100.0%	77.78%	95.42%	89.44%	100.00%
200	86.7%	98.8%	79.72%	95.00%	89.44%	99.58%
100	85.6%	99.6%	78.06%	94.17%	87.50%	97.50%
50	82.5%	94.6%	73.61%	87.08%	80.56%	96.67%
40	78.1%	90.8%	70.56%	84.17%	78.89%	93.75%
30	76.1%	89.2%	64.72%	75.83%	69.72%	85.42%
20	65.8%	75.4%	57.78%	68.75%	64.44%	79.17%
10	52.2%	60.0%	42.50%	52.92%	56.94%	71.25%

Table 4.2. - Performance of the Bayes Quadratic Discriminant for Four Class and Six Class Problem versus the Record Length

Input Data Record Length (ms)	Subject #1		Subject #2		Subject #3	
	Average 6 classes	Average 4 classes	Average 6 class	Average 4 class	Average 6 classes	Average 4 classes
1024	93.1%	99.2%	81.39%	97.50%	95.00%	100.00%
512	92.5%	99.6%	82.50%	95.83%	94.72%	100.00%
256	91.1%	98.8%	79.44%	94.58%	93.33%	98.75%
200	91.4%	99.2%	82.78%	93.33%	91.94%	97.92%
100	87.5%	97.5%	83.33%	94.17%	89.17%	95.00%
50	84.7%	95.0%	70.83%	81.67%	81.94%	94.58%
40	81.4%	92.9%	65.56%	75.83%	78.61%	92.92%
30	76.4%	85.8%	63.89%	70.00%	68.89%	81.67%
20	65.8%	74.6%	54.72%	59.17%	62.22%	73.75%
10	47.5%	55.4%	44.72%	52.50%	49.44%	62.50%

Table 4.3. - Performance of the Linear Discriminant for Four Class and Six Class Problem versus the Record Length

Input Data Record Length (ms)	Subject #1		Subject #2		Subject #3	
	Average 6 classes	Average 4 classes	Average 6 class	Average 4 class	Average 6 classes	Average 4 classes
1024	85.8%	97.5%	85.83%	98.33%	84.44%	96.25%
512	84.4%	97.5%	86.94%	96.25%	85.28%	94.17%
256	85.3%	97.1%	83.06%	93.33%	81.11%	92.08%
200	85.6%	96.7%	80.56%	92.08%	81.67%	91.25%
100	83.3%	95.4%	79.44%	89.58%	77.78%	87.50%
50	84.4%	95.4%	70.56%	78.75%	72.22%	80.42%
40	82.8%	92.5%	68.61%	78.75%	66.11%	76.67%
30	78.3%	87.5%	63.33%	72.92%	62.22%	72.08%
20	72.2%	80.0%	55.56%	65.00%	52.50%	62.50%
10	50.6%	60.0%	39.17%	46.25%	43.06%	48.33%

Table 4.4. - Performance of the Minimum Distance for Four Class and Six Class Problem versus the Record Length

As seen from the tables, the performance of each classifier improved by approximately 10% for all subjects when the problem was reduced to four classes. The classification accuracy of Subject #2 with 1024 ms of MES data was improved from 80-85% for six class problem to 98-99% when the two confused classes were removed. And, the classification accuracy was improved from 70-74% to 79-87% even with only 50 ms of MES data when four classes were considered. The performance of Subject #3 is similar. A classification accuracy (84-95% with 1024 ms data) improved to 96-100% when four classes were considered. Furthermore, the performance of Subject #3 with four classes is 96.7% even with 50 ms of MES data (the Bayes quadratic discriminant was used). These results show that the proposed strategy can identify patterns in the MES with a high classification accuracy even when the data record is short.

4.5. Tracking

To show that the proposed strategy can be used as a continuous type of control, a tracking scheme was devised. Six different hand movements with ten seconds per activity for a total of one minute of motion were performed by the subjects.

Again, the same three classifiers were used to test the scheme. The steady-state data was used as the training set, while the dynamic data was the test set. A sample of the dynamic data is shown in Figure 4.23. The record length of the input data was varied from 1024 to 10 ms with a 50% window overlap.

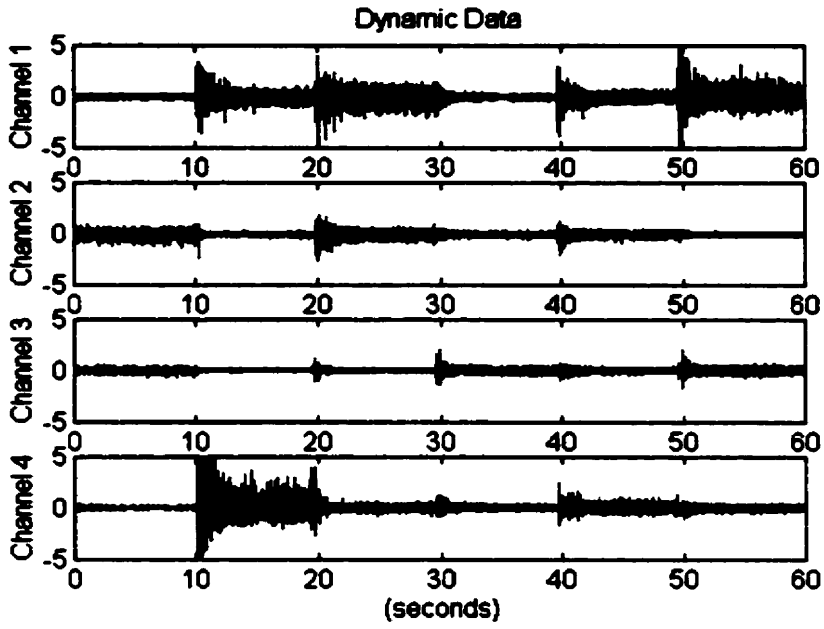

Figure 4.23. - A Sample of the Dynamic Data

Figures 4.24a, 4.24b, 4.24c, and 4.24d demonstrate results of the strategy when the Bayes quadratic discriminant (Q. D.) classifier is used to track the dynamic data. Figure 4.24a shows the output of the classifier when 1024 ms with 512 ms overlap used as the input data to track the changes. This means that the decision was made every M samples based on the previous 2M samples (i.e. 50% overlap). The strategy tracked the changes with average classification error for six classes (hand movements) of 17.0%. Figure 4.24b shows the tracking result when the data of 256 ms with 128 ms window was used. The error rate is 18.0%. Figure 4.24c shows the output when the input data used 100 ms and Figure 4.24d displays the result as the input data employed was 50 ms. The average classification error are 15.6% and 15.8% respectively. The average error rate for shorter data record is lower because the shorter the data record duration, the more iterations available for a given data record length (10 seconds for each movement) which

results in lower percentage error (i.e. 5/100 is less than 1/16). The results shown were excerpted from the best subject for the Bayes quadratic discriminant. Other results with other record lengths are included in Appendix C (CD-ROM).

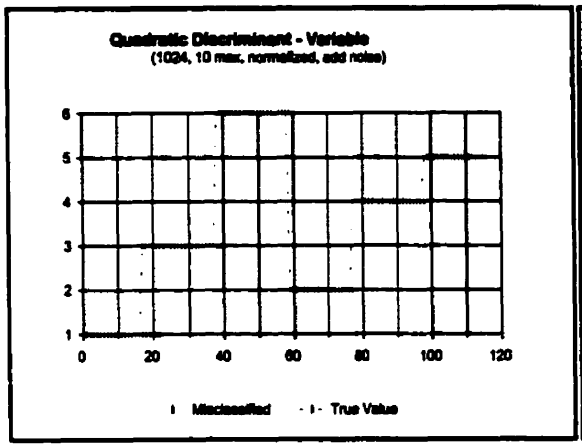

Figure 4.24a. - Tracking Result using Q. D. with the Input Data of 1024 ms

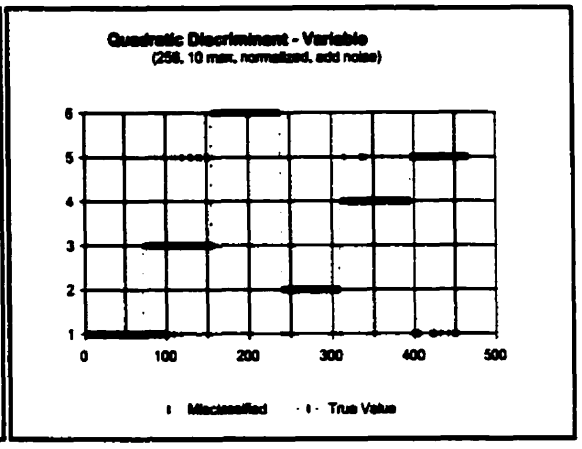

Figure 4.24b. - Tracking Result using Q. D. with the Input Data of 256 ms

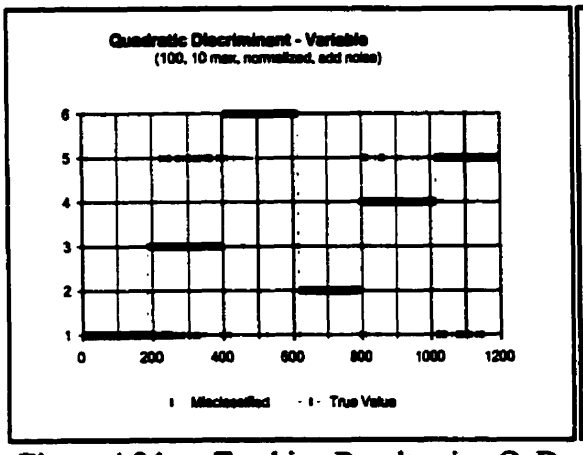

Figure 4.24c. - Tracking Result using Q. D. with the Input Data of 100 ms

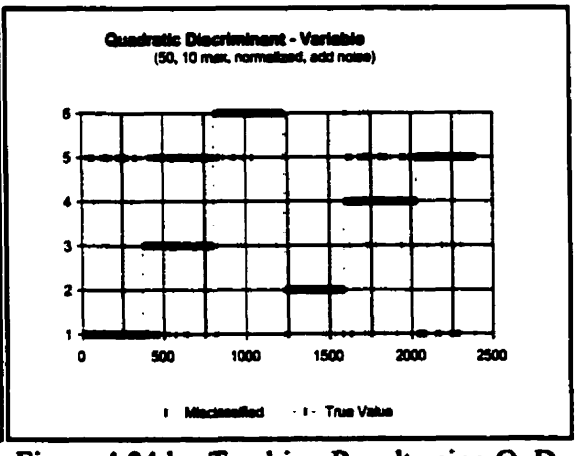

Figure 4.24d. - Tracking Result using Q. D. with the Input Data of 50 ms

Figures 4.25a, 4.25b, 4.25c, and 4.25d demonstrate results of the strategy when the linear discriminant (L. D.) classifier was employed to track the dynamic data with 1024, 256, 100, and 50 ms respectively. Again, 50% of the input data record length was

used as the overlap window. The average classification error for six classes are 9.0%, 4.4%, 7.0% and 13.8% respectively. Those results were taken from the best subject.

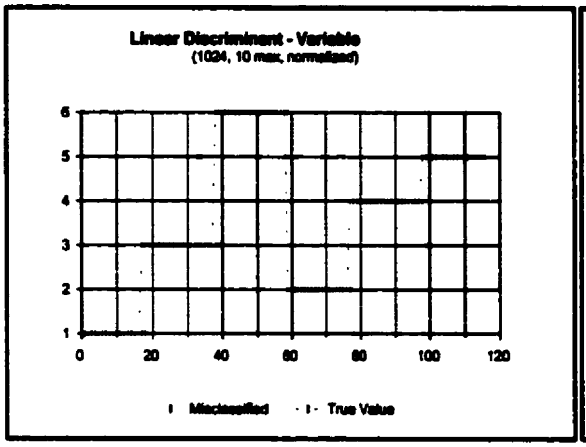

Figure 4.25a. - Tracking Result using L. D. with the Input Data of 1024 ms

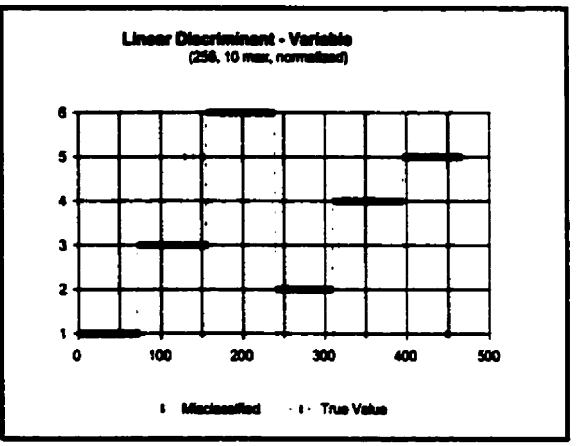

Figure 4.25b. - Tracking Result using L. D. with the Input Data of 256 ms

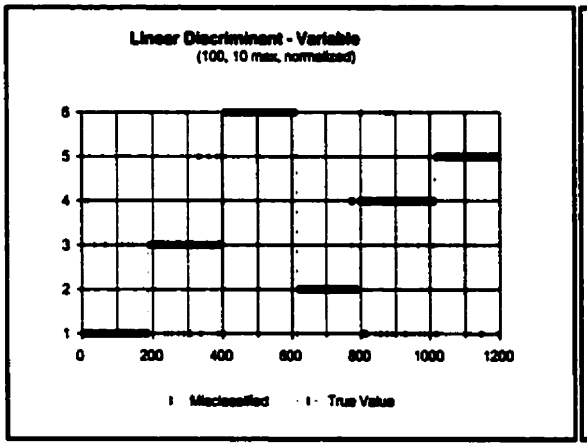

Figure 4.25c. - Tracking Result using L. D. with the Input Data of 100 ms

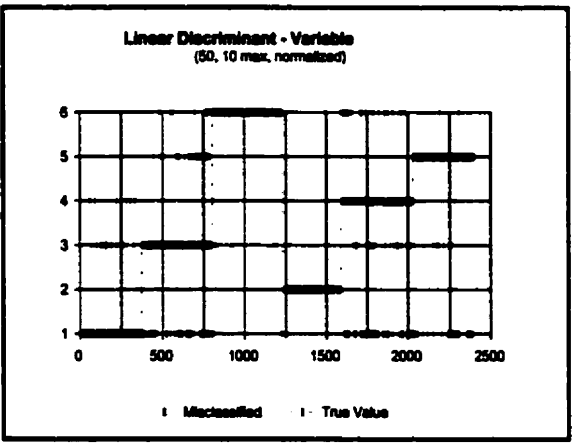

Figure 4.25d. - Tracking Result using L. D. with the Input Data of 50 ms

The results of the minimum distance (M. D.) classifier tracking the dynamic data with 1024, 256, 100 and 50 ms record length are shown in Figures 4.26a, 4.26b, 4.26c, and 4.26d respectively. The overlap window is 50% of the input data record length. The average classification error of the minimum distance classifier shown in the figures while

tracking the dynamic data are 12.4%, 10.2%, 12.5%, and 16.5%. Those results were selected from the best subject.

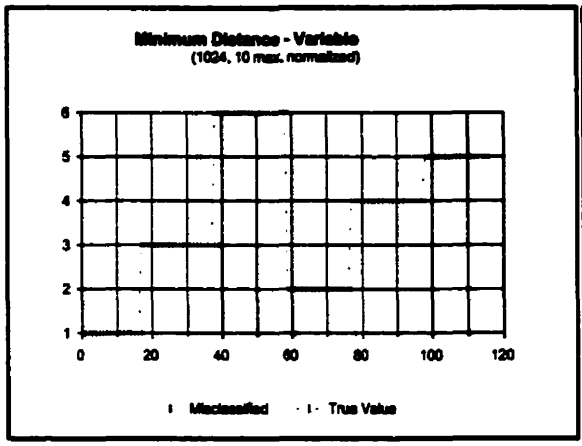

Figure 4.26a. - Tracking Result using M. D. with the Input Data of 1024 ms

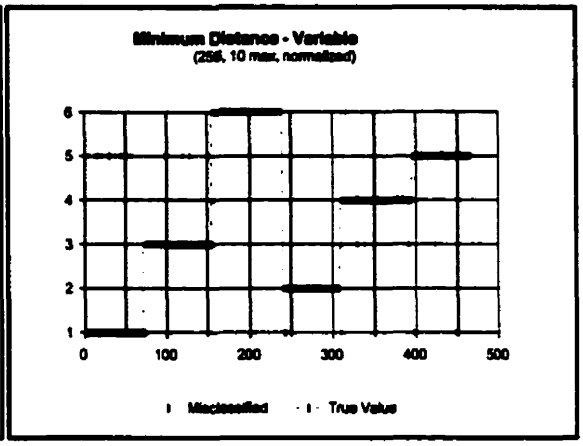

Figure 4.26b. - Tracking Result using M. D. with the Input Data of 256 ms

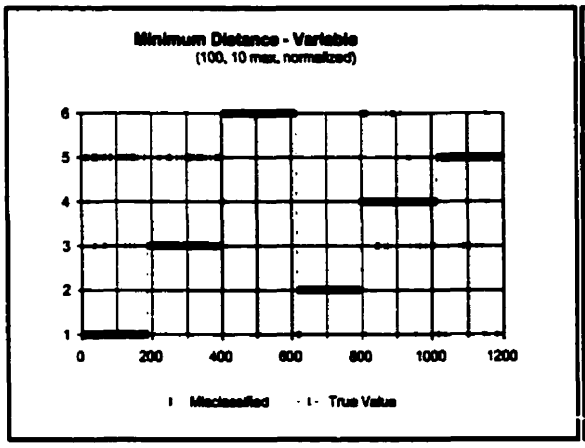

Figure 4.26c. - Tracking Result using M. D. with the Input Data of 100 ms

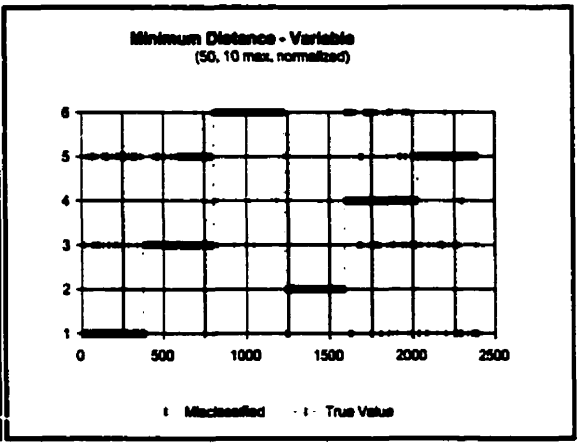

Figure 4.26d. - Tracking Result using M. D. with the Input Data of 50 ms

Table 4.5 shows the average error rate of each classifier tracking the dynamic data. The first column represents the record length of the data input. The second, fourth, and sixth columns show the error rate of the best subject for each classifier. The third, fifth, and seventh columns summarize the average error rate of each classifier over all subjects

tracking six classes of the dynamic data.

Input Data Record Length (ms)	Error Rate for Six Classes					
	Quadratic Discriminant		Linear Discriminant		Minimum Distance	
	(a)	(b)	(a)	(b)	(a)	(b)
1024	17.0%	24.6%	9.0%	22.9%	12.4%	28.8%
512	14.2%	23.0%	4.8%	23.1%	10.3%	27.6%
256	18.0%	35.4%	4.4%	26.4%	10.2%	29.1%
200	17.4%	40.4%	3.6%	31.5%	10.6%	34.1%
100	15.6%	37.7%	7.0%	33.5%	12.5%	36.3%
50	15.8%	37.6%	13.8%	38.8%	16.5%	40.6%
40	15.7%	38.8%	14.2%	40.8%	17.7%	43.0%
30	22.3%	39.8%	18.3%	42.5%	23.7%	45.0%
20	28.6%	44.6%	24.3%	45.2%	30.8%	48.3%

Table 4.5. - Average Error of The Dynamic Data for Six Movements of (a) the best subject, (b) average over all subjects

Although Table 4.5 shows that the classification rate decreases as the data is reduced, the best subject can track the six classes of the dynamic data with less than 20% error even with 40 ms of MES data. This means that the decision was made every 20 ms which is faster than the mechanical response of the current MEC systems (a decision is made every M samples for every 2M samples). The results show that this strategy can be used by some individuals to continuously track the changes exhibited by the MES data. The average error in this case is approximately 40% which means that for most individuals, six class problem is perhaps too complex. A reduced four class problem would certainly improve the performance and lower the classification error.

Whether the performance can be improved when (1) more electrodes are used, and (2) the window overlap is changed, is still unknown. These options and other possibilities are left for future work.

Chapter 5

Conclusions and Future Work

5.1. Summary

It was noted that current multifunction MEC systems require at least 200 ms of MES data to select a function with an acceptable classification rate. This is a major hindrance to the development of a continuous type of control. The purpose of this thesis was to determine if the time to select a function can be reduced while maintaining an acceptable classification accuracy. Chapter 1 introduced the background, stated the problem, presented the thesis objectives, and outlined the topics for each chapter. Chapter 2 provided additional background on the MES, relevant literature review on MEC, the evolution of MEC and reasons for employing an electrode array. Chapter 3 formulated and presented a new strategy for MEC which uses an array of surface electrodes and a correlation feature vector, $\bar{Z}(m)$. It also demonstrated the performance of the strategy in which it was able to classify three distinct patterns with greater than 90% accuracy with only 30 ms data on a simple set of simulated MES data. Chapter 4 presented results of the strategy when it was tested on real MES data. The transient and the steady-state data were tested using different variable combinations (i.e. threshold window size, correlation feature vector $\bar{Z}(m)$, and data record length) on three different classifiers. When tested with transient data, the strategy achieved an average of 85% classification accuracy with 256 ms of MES data. The result is comparable to current MEC systems that use transient

MES data. It also demonstrated that 200 ms of MES data seems to be the minimum time required to capture sufficient information to extract distinct patterns in the transient data. When tested with steady-state data, the strategy was able to classify six classes with an average of 90% classification accuracy with 256 ms and an average of 85% classification accuracy with as little as 50 ms of MES data. This performance performs same strategy on the transient data as shown by Hudgins. However, the current strategy uses a different set, different class, and different thresholding techniques to capture the transient pattern. When the problem was reduced to classify four classes, the performance of the strategy significantly improved (over 10%). Section 4.5 also demonstrated the ability of the strategy to track dynamic movements as the data was shortened.

5.2. Discussion

Early myoelectric control systems such as the three-state UNB systems can be modified to provide continuous control. However, these systems are limited to one or two functions. Newer systems such as those based on pattern recognition (i.e. Hudgins', Graupe) were developed to increase the functionality of the MEC. Unfortunately, although the number of controlled functions were indeed increased, these systems forced a time delay between function selections which hinders their use for continuous control. Therefore, the new strategy outline in this thesis was proposed to reduce the time delay between switching between functions in the multifunction MEC systems.

As demonstrated in this thesis, the new strategy uses a correlation feature vector extracted from an array of surface electrodes. The information from the electrode array

provides a broader and more complete measure of MES characteristics than the information measured from a single site. The correlation feature vector is employed to efficiently capture both within channel (autocorrelation) and across channel (cross-correlation) information from every channel of the array. This exploits the existence of crosstalk which has different characteristics from different contraction conditions.

In this thesis the array consisted of four signal channels. This work has shown that this arrangement was sufficient to capture information to classify six basic hand movements with a high degree of success. However, the number of myoelectric channels is not limited to four channels. When more complex movements are to be classified, the channels can be increased to allow a greater capture of the signal and to enrich the information of the feature vector.

5.3. Conclusion

The new strategy takes advantages of the information captured by the array of surface electrodes and features exhibited by the autocorrelation and the cross-correlation to extract patterns in the myoelectric signal. It exploits the existence of the crosstalk and using all the information it gathers from an active site, including crosstalk, the new strategy increases the speed of decision making and subsequently the response time. The results show that the strategy can make a reasonable decision with only 50 ms of the steady-state myoelectric signal data.

5.4. Original Contribution

In the author's opinion, the original contribution of this research is:

for the first time, to the knowledge of the author, a myoelectric control strategy can extract patterns in the MES with a reasonable accuracy with as little as 50 ms myoelectric signal data. The decision time is faster than the mechanical response of the existing powered prostheses.

5.5. Recommendation and Future Work

As in any field, the introduction of a new concept often brings more questions than answers. The following future work is recommended:

1. Extend the work of Chapter 4 to test the strategy on more subjects which should include amputee subjects.
2. Investigate the effect of increasing the number of myoelectric channels. The results shown are for four myoelectric channels. The addition of more channels may capture more information which could result in more distinct patterns.
3. Determine the optimum positions of the electrode array.
4. Investigate performance sensitivity to array displacement. A preliminary result of the sensitivity test is presented in Appendix A.
5. Develop more advanced classifiers such as neural networks to test the strategy.
6. Develop an algorithm to detect the initiation point of the transient MES data.
7. Implement the hardware so that clinical testing of the strategy can be carried out in real time.

References

1. Basmajian, John V., and Carlo J. De Luca, **"Muscles Alive: Their Functions Revealed by Electromyography"**, 5th ed., Baltimore: Williams and Wilkins, 1985.
2. Plonsey, R. And Roger C. Barr, **"Bioelectricity : a Quantitative Approach"**, New York: Plenum Press, 1991.
3. Starkermann, R., **"A New Electrohand"**. Original article: Reiter, von Reinhold, **"Eine Neue Elektrokunsthand"**, *Grenzgebiete der Medizin*, vol. 1, no. 4, 1948, 133-135.
4. Simpson, D. C., **"The Control of a Multi-Movement Powered Upper Limb Prosthesis"**, *The European Symposium on Med. Elec.*, part 2, September 28 - October 1, 1965.
5. Kobrinsky, A. Ye., **"Bioelectrical Control of Prosthetic Devices"**, *U.S. Joint Publications Research Service*, 18 November 1960.
6. Dorcas, D. S., and R. N. Scott, **"A Three-State Myoelectric Control"**, *Med. and Biol. Eng.*, vol. 4, no. 4, 1966, 367-370.
7. Hudgins, Bernard S., **"A New Approach to Multifunction Myoelectric Control"**, *Ph.D. Thesis, University of New Brunswick*, 1991.
8. Katz, B., **"Nerve, Muscle and Synapse"**, New York: McGraw-Hill, 1966.
9. Parker, P. A., **"Optimum Signal Processing for a Multifunction Myoelectric Communication Channel"**, *Ph.D. Thesis, University of New Brunswick*, 1975.

10. DeLuca, C. J., **"Physiology and Mathematics of Myoelectric Signals"**, *IEEE Trans. on Biomed. Eng.*, vol. BME-26, April 1979, pp. 313-325.

11. Kreifeld, J. G., and S. Yao, **"A Signal-to-Noise Investigation of Nonlinear Electromyographic Processors"**, *IEEE Trans. on Biomed. Eng.*, vol. BME-21, no. 4, March 1974, pp. 298-308.

12. Hogan, N. J., **"Myoelectric Prosthesis Control: Optimal Estimation Applied to EMG and the Cybernetic Considerations for Its Use in a Man-Machine Interface"**, *Ph.D. dissertation*, M.I.T., Cambridge, Massachusetts, 1976.

13. Cunningham, E. A., and N. Hogan, **"Effects of Tissue Layers on The Surface Myoelectric Signal"**, *IEEE 1981 Frontiers of Eng. in Health Care*, 1981, 3-7.

14. Merletti, R., and L. R. Lo Conte, **"Advances in Processing of Surface Myoelectric Signals: Part 1"**, *Med. & Biol. Eng. & Comp.*, vol. 33, no. 3, May 1995, 362-372.

15. Lo Conte, L. R., and R. Merletti, **"Advances in Processing of Surface Myoelectric Signals: Part 2"**, *Med. & Biol. Eng. & Comp.*, vol. 33, no.3, May 1995, 373-384.

16. Hammond, P.H., **"The Control of Artificial Limbs"**, Discovery, London, vol. 27, March 1966, 21-25.

17. Wan, E. A., Kovacs, G. T. A., Rosen, J. M., and B. Widrow, **"Development of a Neural Network Interface for Direct Central Nervous Control of a Prosthetic Limb"**, *Proc. Intl. Joint Conf. on Neural Networks*, Washington D.C. - USA, 1990, II-3-II-21.

18. Scott, R. N., and P. A. Parker, **"Myoelectric Prostheses: State of the Art"**, *Jour. of Med. Eng. & Tech.*, vol. 12, no. 4, 1988, 143-151.

19. Parker, P. A., Scott, R. N., and Y. T. Zhang, **"Background Noise in Myoelectric Channel: Effect on SNR of ME Signals"**, *Proc. 15th Annual Northeast BioEng. Conf.*, Boston - USA, 1989, 237-238.

20. Godin, D. T., Parker, P. A., and R. N. Scott, **"Noise Characteristics of Stainless-Steel Surface Electrodes"**, *Med. & Biol. Eng. & Comp.*, vol. 29, no. 6, November 1991, 585-590.

21. Childress, D. A., **"A Myoelectric Three State Controller using Rate Sensitivity"**, *Proc. 8th Intl. Conf. in Med. and Biol. Eng.*, Chicago - USA, 1969, 4-5.

22. Englehart, Kevin B., **"Signal Representation for Classification of the Transient Myoelectric Signal"**, *Ph.D. Thesis, University of New Brunswick*, 1998.

23. Saridis, G. N., and T. P. Gootee, **"EMG Pattern Analysis and Classification for a Prosthetic Arm"**, *IEEE Trans. on Biomed. Eng.*, vol. BME-29, no. 6, June 1982, 403-412.

24. Hudgins, Bernard S., Parker, P. A., and Robert N. Scott, **"A New Strategy for Multifunction Myoelectric Control"**, *IEEE Trans. on Biomed. Eng.*, vol. 40, no. 1, January 1993, 82-94.

25. Hudgins, Bernard S., Parker P. A., and Robert N. Scott, **"Control of Artificial Limbs using Myoelectric Pattern Recognition"**, *Med. & Life Sci. Eng.*, vol. 13, 1994, 21-38.

26. Scott, R. N., **"Myoelectric Energy Spectra"**, *Med. & Biol. Eng.*, vol. 5, 1967, 303-305.

27. Graupe, D., and W. K. Cline, **"Functional Separation of EMG Signals via ARMA Identification Methods for Prosthesis Control Purposes"**, *IEEE Trans. Systems, Man, Cybernetics*, vol. SMC-5, no. 2, March 1975, 252-259.

28. Graupe, D., Magnussen, J., and A. Beex, **"A Microprocessor System for Multi functional Control of Upper Limb Prostheses via Myoelectric Signal Identification"**, *IEEE Trans. on Auto. Contr.*, vol. AC-23, August 1978, 538-544.

29. Englehart, K., Hudgins, B., Parker, P. A., and M. Stevenson, **"Time-Frequency Methods for Classification of the Transient Myoelectric Signal"**, *Proc. 12th Congress of the Intl. Soc. of Electrophysiology and Kinesiology*, Montreal - Canada, 1998, 22-23.

30. Masuda, T., **"A Reliable Myoelectric Signal Detector Based on the Propagation Characteristics of Motor Unit Action Potentials"**, *IEEE Trans. on Biomed. Eng.*, vol BME-33, no. 9, September 1986, 876-878.

31. Reucher, H., Rau, G., and Jiri Silny, **"Spatial Filtering of Noninvasive Multielectrode EMG: Part I - Introduction to Measuring Technique and Applications"**, *IEEE Trans. on Biomed. Eng.*, vol. BME-34, no. 2, February 1987, 98-105.

32. Reucher, H., Silny J., and Gunter Rau, **"Spatial Filtering of Noninvasive Multielectrode EMG: Part II - Filter Performance in Theory and Modeling"**, *IEEE Trans. on Biomed. Eng.*, vol. BME-34, no. 2, February 1987, 106-113.

33. Papakyriakou, M. J., Parker, P. A., and R. N. Scott, **"Measurement of Muscle Fiber Conduction Velocity using Surface EMG"**, *Proc. 9th Annual Conf. IEEE Eng. in Med. and Biol. Soc.*, Boston - USA, 1987, 331-332.

34. Rau, G., Silny, J., and J. Schneider, **"Muscular Conduction Velocity Detected NonInvasively by a Spatial Filtering Multi-Lead Electrode Array"**, *Proc. 9th Annual Conf. IEEE Eng. in Med. and Biol. Soc.*, Boston - USA, 1987, 339-340.

35. Harba, M. I. A., Zaia, I. F., and A. K. Naief, **"On-line Measurement of Muscle Fibre Conduction Velocity: Analysis and Optimization of Performance"**, *Jour. Biomed. Eng.*, vol. 10, January 1988, 33-45.

36. Hogan, N., and R. W. Mann, **"Myoelectric Signal Processing: Optimal Estimation Applied to Electromyography - Part I: Derivation of The Optimal Myoprocessor"**, *IEEE Trans. on Biomed. Eng.*, vol. BME-27, July 1980, 382-395.

37. Hogan, N., and R. W. Mann, **"Myoelectric Signal Processing: Optimal Estimation Applied to Electromyography - Part 2: Experimental Demonstration of Optimal Myoprocessor Performance"**, *IEEE Trans. on Biomed. Eng.*, vol. BME-27, July 1980, 396-410.

38. Clancy, Edward A., and Neville Hogan, **"Multiple Site Electromyograph Amplitude Estimation"**, *IEEE Trans. on Biomed. Eng.*, vol. 42, no. 2, February 1995, 203-211.

39. Doerschuk, Peter C., Gustafson, Donald E., and Alan S. Willsky, **"Upper Extremity Limb Function Discrimination using EMG Signal Analysis"**, *IEEE Trans. on Biomed. Eng.*, vol. BME-30, no. 1, January 1983, 18-29.

40. Gray, H., **"Gray's Anatomy"**, edited by: T. Pickering Pick and Robert Howden, 15th ed., New York: Barnes & Noble Books, 1995, 350-392.

41. Papoulis, A., **"Signal Analysis"**, Montreal: McGraw-Hill, 1977.

42. Haykin, S., **"Adaptive Filter Theory"**, 2nd ed., Toronto: Prentice-Hall, 1991.

43. Hunt, James A., **"A 3-Degree-of-Freedom Myoelectric Control Suitable for Easy Implementation in Hardware"**, *M.Sc.E. thesis, University of New Brunswick*, 1998.

44. Bezdek, James C., **"Pattern Recognition with Fuzzy Objective Function Algorithms"**, New York: Plenum Press, 1987.

45. Bezdek, James C., and Sankar K. Pal, **"Fuzzy Models for Pattern Recognition:** *Methods That Search for Structures in Data*", New York: IEEE Press, 1992.

Appendix A

Test of sensitivity

It has been reported that one of the drawbacks of employing an electrode array is the difficulty in repeatedly placing it in the same location [36], [37], [39]. Since an array is sensitive to the displacement due to the different pickup regions, consistent myoelectric signals are difficult to obtain. The purpose of this test was to determine how much the new strategy suffers when the location of the array is moved.

Three subjects participated in the test. They were asked to return to the laboratory one week after the original set of data was collected. The electrodes were placed 0.5-2 cm laterally from the original positions. The subjects were asked to perform the same six basic hand movements. Although both steady-state and transient data were collected and analyzed, only the steady-state output is presented here.

Again, three classifiers (the Bayes quadratic discriminant, the linear discriminant, and the minimum distance) were used in the analysis. Figures A.1a, A.2a, and A.3a show the results of each classifier when the record length of the training set equaled 1024 ms and the record length of the test set was varied from 1024 to 10 ms. Figures A.1b, A.2b, and A.3b display the results of each classifier when the record length of the training set was varied to match with the data length of the test set.

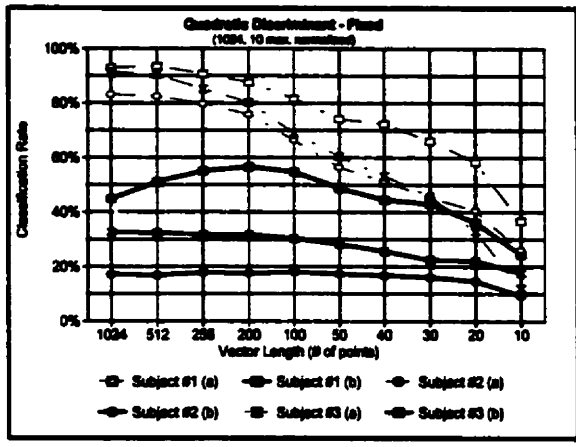

Figure A.1a. - Q. D. Classification Rate using Fixed Length Training Set

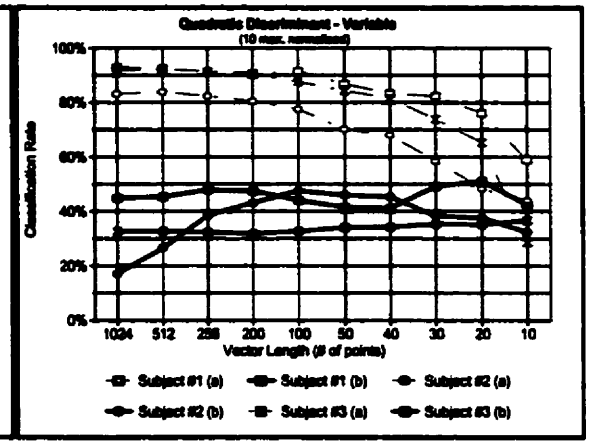

Figure A.1b. - Q. D. Classification Rate using Variable Length Training Set

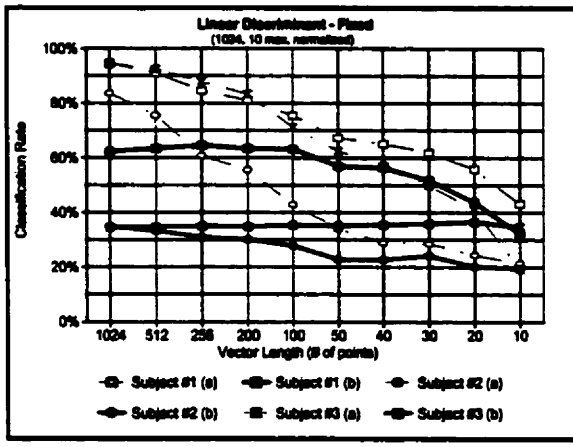

Figure A.2a. - L. D. Classification Rate using Fixed Length Training Set

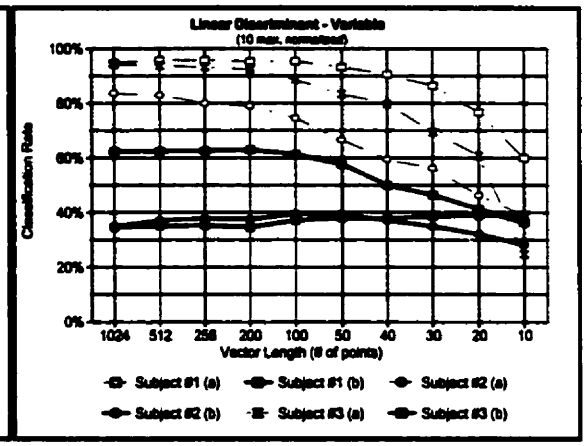

Figure A.2b. - L. D. Classification Rate using Variable Length Training Set

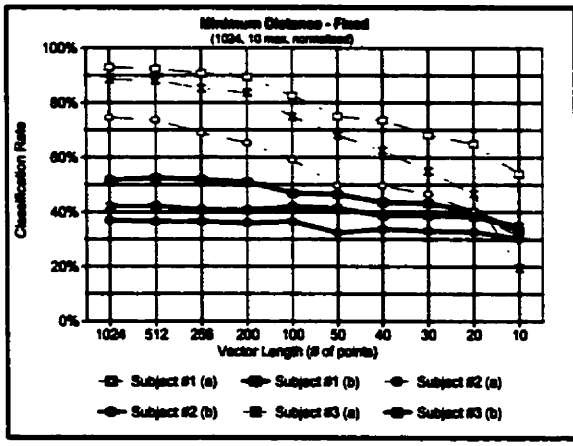

Figure A.3a. - M. D. Classification Rate using Fixed Length Training Set

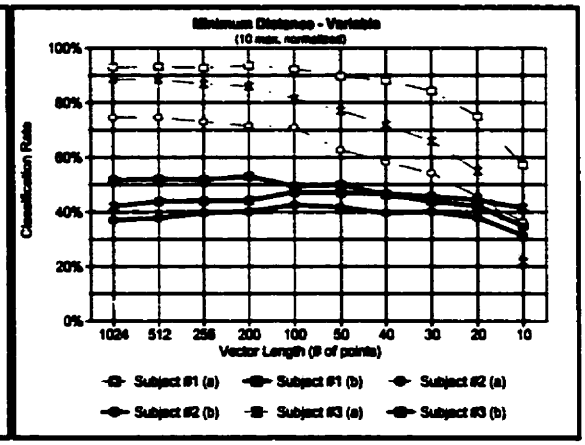

Figure A.3b. - M. D. Classification Rate using Variable Length Training Set

In the legends of each figure, Subject #1 (a), Subject #2 (a), and Subject #3 (a) represent the average performance of two data sets (show by dashed lines). The legends of Subject #1 (b), Subject #2 (b), and Subject #3 (b) represent the results of the sensitivity test where the first data set was used as the training set and the second data set was used as the test set.

The results showed that the array is very sensitive to changes in its location. Only major classes could be identified correctly. The minor classes were completely masked by major classes. A clearer look at how the minor classes were totally covered by the major classes can be seen from the confusion matrices (included in Appendix C on CD-ROM). The results show that, out of six classes (hand movements), only two could be reasonably identified. Two movements were 50% misclassified, and the remaining two were completely misclassified. As a result of this, the error rate was very high.

Since the test was done in the worst case (by purposely moving the location of the electrodes), the success of recognizing four classes showed that the strategy was not a total failure. Furthermore, current technology allows a very tight and precise socket placement which can restrict the electrodes to a small displacement (< 1cm). However, further studies on this sensitivity issue must be carried out before the strategy can be implemented.

Appendix B

A sample of a consent form and the letter of correspondence are included in the following two pages. Each subject read and signed the consent form and answered the additional information asked in the letter of correspondence.

Informed Consent Form

Title: Investigation of an Array of Electrodes on Myoelectric Signals

Researchers: Supervisors: Bernard Hudgins, Ph.D.
Philip A. Parker, Ph.D.
Investigator: Sentiono Leowinata, B.Sc.

Purpose:

The purpose of this experiment is to investigate whether an array of electrodes has more advantages in capturing myoelectric signal from the skin surface than the ordinary two channels configuration of electrodes. The array of electrodes is to record from the skin surface the electrical signals as a result of the activities of the above elbow muscles such as biceps and triceps.

The signals obtained will be used to develop and to evaluate enhancement for myoelectric control prostheses. The information captured, if it is proven successful, is an important step to achieve simultaneous control of an artificial prosthetic limb.

Procedure:

A small area around the upper arm where the electrodes are placed will be treated. As part of skin preparation, the stratum corneum (that is the dead upper layer of the skin surface) will be removed carefully using a soft sand paper and then followed by treating it with alcohol. An array of electrodes which consist of four surface electrodes in an elastic band will be placed on around the upper arm where the area has been cleaned.

The subject is asked to produce a normal muscle contraction. The signals produced will be captured by the electrodes. The electrodes are connected to electronic instrumentation which amplify and record the signals for further analysis.

Risk:

As any other experimental procedure, there is a very small risk associated with electrical shock. Every precautions and possible steps have been considered to keep the subject as safe as possible by using opto-isolator to isolate the electronic instrumentations from the subject.

Withdrawal:

The subject is free to withdraw from the experiment at any time without any obligation.

I,_____certify that I have read and understood the above explanation of the research procedure and all of my questions have been answered to my satisfaction.

Signature :_____

Witness :_____ Signature:_____

Date :_____(mo/dt/yr)

Appendix I

Dear (name inserted),

Thank you for your interest to participate in the experiment. I really appreciate your help.

Please allow me to explain the purpose of the experiment. The purpose of this experiment is to investigate whether an array of electrodes can obtain more signals than the standard/usual configuration (use two pairs of electrodes). Until today, the idea of simultaneous myoelectrically controlled artificial limbs is up in the air because insufficient number of inputs can be obtained from the muscle. This experiment will try to reduce the gaps and make the dream come true. Your participation will give a chance to reach this goal.

The experiment will be conducted inside the Institute of Biomedical Engineering building, a building below the bookstore, inside University of New Brunswick, Fredericton campus.
I would like to get more information from you and schedule the time to perform the experiment.

Name :
Age :
Sex :

Do you have any allergic reactions with rubber?	Yes	No
Do you have any allergic reactions with alcohol (not to drink, just rubbing)?	Yes	No
Do you have any anomalies or any diseases related to upper arm muscles?	Yes	No
Can you perform normal functional movements such as touching the nose, the ear or the lips, contracting/extending your arm?	Yes	No
Have you ever performed similar experiments (recording upper arm myoelectric signals with surface electrodes)?	Yes	No

Is there anything you would like to add? (especially regarding to your health or prior experience with this type of research)

_____

_____

What is good time for you to perform the experiment?

Thank you very much and if you have any other questions, please do not hesitate to ask.
Sincerely yours,
Sentiono Leowinata
Fredericton-NB-Canada, c5ip@unb.ca, 506-458-7889

Ps. Please note that you are free to withdraw at any time without any obligations if the experiment is not as you expected.

Appendix C

List of CD-ROM Contents

The CD-ROM is logically divided into three main directories. The first directory consists of the data used in the experiment. The second directory contains template of MATLAB scripts. The third directory holds the results of all calculation performed.

DATA

The data of subjects is broken into four parts: the dynamic data, the simulated data, the steady-state data, and the transient data.

Dynamic data sub-directories (please read the readme.txt file):

\Data\Dynamic\Subject1 - \Data\Dynamic\SubjectB

Simulated data file:

\Data\Simulated\rawdata.dat

Steady-State data sub-directories (please read the readme.txt file):

\Data\Steady\Subject1 - \Data\Steady\SubjectC

Transient data sub-directories (please read the readme.txt file):

\Data\Transient\Subject1 - \Data\Transient\SubjectC

MATLAB SCRIPTS

The scripts is divided into three main directories, according to the data: the simulated data, the steady state data, and the transient data.

The simulated data contains the following sub-directories: Bayes Quadratic Discriminant (3.2.2.3), Fuzzy c-Means (3.2.2.4), Minimum Distance (3.2.2.2) and Rank Order

(3.2.2.1). The Bayes Quadratic Discriminant and the Minimum Distance directories are also divided further. Please check the respective directories as they are self explanatory.

The steady state data directory is divided into few sub-directories: Four Class Classification (4.4), Performance Measure (4.3.2.2), Six Class Classification (4.3.2.1), Test of Sensitivity (Appendix A), Tracking Dynamic Data (4.5). Each directory contains few sub-directories.

The transient data directory is divided into 3 main sub-directories: Bayes Quadratic Discriminant, Linear Discriminant and Minimum Distance. Each directory again divided into two main sub-directories: 10-Feature Vector and 16-Feature Vector. The transient data directory gives scripts samples of section 4.3.1.

RESULTS

Results that cannot be included in the thesis can be found in this CD-ROM. The results are categorized into 5 main sub-directories: Four-Class (4.4), Sensitivity (Appendix A), Steady-State (4.3.2), Tracking (4.5), and Transient (4.3.1).